

General Disclaimer

One or more of the Following Statements may affect this Document

- This document has been reproduced from the best copy furnished by the organizational source. It is being released in the interest of making available as much information as possible.
- This document may contain data, which exceeds the sheet parameters. It was furnished in this condition by the organizational source and is the best copy available.
- This document may contain tone-on-tone or color graphs, charts and/or pictures, which have been reproduced in black and white.
- This document is paginated as submitted by the original source.
- Portions of this document are not fully legible due to the historical nature of some of the material. However, it is the best reproduction available from the original submission.



SSME INTERSTAGE SEAL RESEARCH

PROGRESS REPORT
Contract NAS8-33716

Prepared by:

Dara W. Childs, Ph.D., P.E.

January 1984
Report No: RD-1-84

(NASA-CR-170995) SSME INTERSTAGE SEAL
RESEARCH Progress Report (Texas A&M Univ.)
86 p HC A05/MF A01

N84-20631

CSCL 21H

Unclassified
G3/20 12039

Turbomachinery Laboratories
Mechanical Engineering Department

SSME INTERSTAGE SEAL RESEARCH
PROGRESS REPORT-CONTRACT NAS8-33716

Prepared by
Dara W. Childs, Ph.D., P.E.
Professor of Mechanical Engineering

Turbomachinery Laboratories
Mechanical Engineering Department
Texas A&M University
College Station, Texas 77843

Turbomachinery Laboratory
Report No: RD-1-84

January 1984

ABSTRACT

Test results comprising direct and transverse force coefficients and leakage coefficients are reported for six seal configurations. All seals tested use the same smooth rotor and have the same constant minimum clearance. The following stator configurations were tested:

- (a) Smooth,
- (b) Rocketdyne-manufactured knurled pattern,
- (c) axially-grooved pattern with end seals,
- (d) diamond-grid roughened,
- (e) diamond-grid roughened with end seals,
- (f) round-hole pattern.

Comparison of the seals shows the Rocketdyne stator to be the stiffest and the round-hole-pattern stator to yield the largest net damping and the least leakage. The theory of reference [5] is shown to substantially underestimate the stiffness and effective-added-mass coefficients, but do a reasonable job in predicting the net-damping-force coefficient.

PROGRESS REPORT-CONTRACT NAS8-33716

January 1984

Table of Contents

	page
Abstract.	i
List of Figures	ii
List of Tables.	v
Nomenclature.	vii
Introduction.	1
Test Configurations, Capability, and Results.	3
Test Configurations.	3
Test Capability.	3
Test Results	6
Discussion of Results: Comparison to Theory.	7
Introduction	7
Emperical Turbulence Coefficients.	7
Dynamic Test Data.	10
Discussion of Results: Comparison of Stator Configurations . . .	24
Conclusions and Recommendation.	30
References.	31
Appendix A: Analysis and Testing for Rotordynamic Coefficients of Turbulent Annular Seals with Different, Directionally- Homogeneous Surface Roughness Treatments for Rotor and Stator Elements.	32
Appendix B: Test Data Consisting of Operating Conditions and Parameters	49
Appendix C: Test Data Consisting of Force Coefficients and Average Force Magnitudes	63

LIST OF FIGURES

	page
1. Seal test section.	4
2. Rocketdyne-manufactured, knurled-indentation stator insert	4
3. Axially-grooved stator insert with end seals	5
4. Diamond grid stator insert	5
5. Diamond grid stator insert with end seals.	5
6. Round-hole-pattern stator insert	5
7. Measured and finite-length [5] theoretical results for F_r/A and F_θ/A ; smooth stator, $C_r = .394$ mm.	11
8. Measured and finite-length [5] theoretical results for F_r/A and F_θ/A ; Rocketdyne stator, $C_r = .394$ mm.	12
9. Measured and finite-length [5] theoretical results for F_r/A and F_θ/A ; smooth stator, $C_r = .527$ mm.	13
10. Measured and finite-length [5] theoretical results for F_r/A and F_θ/A ; Rocketdyne-knurled stator; $C_r = .527$ mm.	14
11. Measured results for F_r/A and F_θ/A ; axially-grooved stator with end seals.	15
12. Measured and finite-length [5] theoretical results for F_r/A and F_θ/A ; diamond-grid stator.	16
13. Measured results for F_r/A and F_θ/A ; diamond-grid stator with end seals.	17
14. Measured and finite-length [5] theoretical results for F_r/A and F_θ/A ; round-hole-pattern stator.	18
15. C_{ef} versus ΔP for the smooth and Rocketdyne-knurled inserts at $C_r = .394$ mm	24
16. K_{ef} versus ΔP for the smooth and Rocketdyne-knurled inserts at $C_r = .394$ mm	24
17. $C_L \times 1,000$ versus ΔP for the smooth and Rocketdyne-knurled inserts at $C_r = .394$ mm.	25
18. C_{ef} versus ΔP for all stator inserts tested with the minimum radial clearance, $C_r = .527$ mm	26
19. K_{ef} versus ΔP for all stator inserts tested with the minimum radial clearance, $C_r = .527$ mm	26

LIST OF FIGURES (Continued)

List of Tables

	page
1. Emperical turbulence coefficients m_s , n_s for damper seal configurations, and estimates for relative-roughness from Colebrook's formula [9] at $R_a = 300,000$.	9
2. Emperical turbulence coefficients m_o , n_o as calculated from Colebrook's formula [9].	9
3. K_{ef} , C_{ef} , and M_{ef} coefficients from measured and theoretical results; smooth and rocketdyne-knurled stators for $C_r = .394$ and $.527$ mm.	20
4. K_{ef} , C_{ef} , and M_{ef} coefficients from measured and (where appropriate) theoretical predictions for all seals tested which have $C_r = .527$ mm.	22
5. Comparison of stiffness, damping, and leakage characteristics of six stators for $C_r = .527$ mm.	28

Tables: Appendix B

B.1. Test data: Operating conditions and parameters for the smooth stator; $C_r = .3937$ mm.	49
B.2. Test data: Operating conditions and parameters for the Rocketdyne-knurled stator; $C_r = .3937$ mm.	50
B.3. Test data: Operating conditions and parameters for the smooth stator; $C_r = .5271$ mm.	52
B.4. Test data: Operating conditions and parameters for the Rocketdyne-knurled stator; $C_r = .5271$ mm.	54
B.5. Test data: Operating conditions and parameters for the axially-grooved stator; $C_r = .5271$ mm.	56
B.6. Test data: Operating conditions and parameters for the diamond-grid roughened stator; $C_r = .5271$ mm.	58
B.7. Test data: Operating conditions and parameters for the diamond-grid roughened stator with end seals; $C_r = .5271$ mm.	60
B.8. Test data: Operating conditions and parameters for the round-hole-pattern roughened stator; $C_r = .5271$ mm.	62

Tables: Appendix C

	page
C.1. Test data: Force coefficients (average and standard deviations) and average force magnitude for the smooth stator; $C_r = .3937$ mm.	63
C.2. Test data: Force coefficients (average and standard deviations) and average force magnitude for the Rocketdyne-knurled stator; $C_r = .3937$ mm.	65
C.3. Test data: Force coefficients (average and standard deviations) and average force magnitude for the smooth stator; $C_r = .5271$ mm.	67
C.4. Test data: Force coefficients (average and standard deviations) and average force magnitude for the Rocketdyne-knurled stator; $C_r = .5271$ mm.	69
C.5. Test data: Force coefficients (average and standard deviations) and average force magnitude for the axially-grained stator; $C_r = .5271$ mm.	71
C.6. Test data: Force coefficients (average and standard deviations) and average force magnitude for the diamond-grid roughened stator; $C_r = .5271$ mm.	73
C.7. Test data: Force coefficients (average and standard deviations) and average force magnitude for the diamond-grid roughened stator with end seals; $C_r = .5271$ mm.	75
C.8. Test data: Force coefficients (average and standard deviations) and average force magnitude for the round-hole-pattern stator; $C_r = .5271$ mm.	77

NOMENCLATURE

c:	Cross-coupled damping coefficient, introduced in Eq. (1), FT/L.
k:	Cross-coupled stiffness coefficient, introduced in Eq. (1), F/L.
m_r, n_r :	Emperical turbulence coefficients to define the seal-rotor friction factor.
m_s, n_s :	Emperical turbulence coefficients to define the seal-stator friction factor.
A:	Dynamic seal eccentricity, introduced in Eq. (2).
C:	Direct damping coefficient, introduced in Eq. (1), FT/L.
C_{ef} :	Net damping coefficient, introduced in Eq. (8), FT/L.
C_D :	Discharge coefficient, introduced in Eq. (9).
C_L :	Leakage coefficient, introduced in Eq. (10).
C_r :	Minimun seal clearance, L.
F_x, F_y :	Cartesian components of the seal reaction force, introduced in Eq. (1), F.
F_r, F_θ :	Radial and circumferential components of the seal reaction force, F.
K:	Direct seal stiffness coefficient, introduced in Eq. (1), F/L.
M:	Seal added mass coefficient, introduced in Eq. (1), M.
M_{ef} :	Effective seal added-mass coefficient, introduced in Eq. (8), M.
ΔP :	Seal pressure differential, F/L ² .
R:	Seal radius, L.
V:	Average axial fluid velocity in the seal L/T.
X, Y:	Seal displacement components, introduced in Eq. (1), L.
λ :	Seal friction factor, defined in Eq. (4).
$\sigma = \lambda(L/C)$:	Seal friction factor.
ρ :	Seal density, M/L ³ .
ω :	Seal rotational and precessional velocity, T ⁻¹ .
μ :	Seal viscosity, FT/L ² .

INTRODUCTION

The test and analysis results which are reported here were obtained in an extension of NASA Contract NAS8-33716 which was initiated in January of 1980. Earlier contract reports [1, 2, 3] provide detailed information covering the following points:

- (a) seal configurations and test results,
- (b) test-section and facility description,
- (c) test objectives and procedures, and
- (d) data acquisition, analysis, and procedures.

Most of this information is not repeated here, and interested readers are referred to earlier reports.

From a rotordynamics viewpoint, seal analysis has the objective of predicting the coefficients of the following motion/reaction-force model

$$-\begin{Bmatrix} F_X \\ F_Y \end{Bmatrix} = \begin{bmatrix} K & k \\ -k & K \end{bmatrix} \begin{Bmatrix} X \\ Y \end{Bmatrix} + \begin{bmatrix} C & c \\ -c & C \end{bmatrix} \begin{Bmatrix} \dot{X} \\ \dot{Y} \end{Bmatrix} + M \begin{Bmatrix} \ddot{X} \\ \ddot{Y} \end{Bmatrix}, \quad (1)$$

where X, Y are components of the seal rotor relative to its stator and F_X, F_Y are components of the reaction force. The diagonal and off-diagonal stiffness and damping coefficients are referred to, respectively, as "direct" and "cross-coupled". The cross-coupled coefficients arise due to fluid rotation within the seal. The coefficient M accounts for the seal's added mass.

If a circular orbit of the form

$$X = A \cos \omega t, \quad Y = A \sin \omega t \quad (2)$$

is assumed, Eq. (1) yields the following definition of force coefficients which are, respectively, parallel and perpendicular to the rotating displacement vector

$$\begin{aligned} F_r/A &= -K - cw + M\omega^2 \\ F_\theta/A &= k - Cw \end{aligned} \quad (3)$$

Observe that the cross-coupled-stiffness coefficient k yields a "driving" tangential contribution in the direction of rotation, while the direct damping coefficient develops a drag force opposing the tangential velocity.

The present report deals with analysis and test results for five new seal configurations which were largely inspired by von Pragenau's proposed "damper seal" [4] configurations. von Pragenau's analysis predicts that a smooth-rotor/rough-stator combination will yield a reduced asymptotic fluid tangential velocity within the seal, which will, in turn, yield a reduction in the cross-coupled stiffness coefficient. A reduced cross-coupled stiffness coefficient reduces the destabilizing tangential driving force on the rotor, yields an increased net damping force, and generally enhances rotor stability and response. A subsequent and more comprehensive analysis by Childs and Kim [5], which is included as Appendix A, yields the same sort of encouraging predictions.

Test results which are presented include force coefficients (F_r/A and F_θ/A) and leakage rates. Analysis of the test results permits a direct comparison of the stiffness and damping coefficients and leakage characteristics of the seals which have been tested.

TEST CONFIGURATIONS, CAPABILITY, AND RESULTS

Test Configurations

The seal test section is illustrated in figure 1 and was modified by machining out the original test-section housing to create cylindrical seats into which candidate seal stators can be pressed. All seals tested use a smooth rotor and have a constant minimum clearance, i.e., no taper. The following stator configurations were tested:

- (a) smooth,
- (b) Rocketdyne, knurled-indentation pattern,
- (c) axially-grooved pattern with end seals,
- (d) diamond-grid roughened,
- (e) diamond-grid roughened with end seals, and
- (f) round-hole pattern.

The latter five stator configurations are illustrated in figure 2 through 6. Tests were carried out on all seal configurations with the minimum radial clearance $C_r = .527 \text{ mm (.020 in)}$ and seal dynamic eccentricity, $A = .127 \text{ mm (.005 in)}$. In addition, tests were carried out for the smooth and Rocketdyne seals for $C_r = .394 \text{ mm (.015 in)}$; $A = .089 \text{ mm (.0035 in)}$.

Test Capability

The rotor segments of the test seal are mounted eccentrically on the rotor of figure 1 with the eccentricity A . Hence rotor rotation generates a synchronously precessing pressure field. Axially spaced strain-gauge pressure transducers are provided to measure the transient pressure field, and the transient pressure measurements are recorded and integrated to define F_r/A , F_θ/A , and $|F|$. In any test, five to ten cycles of data, containing on the order of 2,000 data points, are analyzed. Each data point yields a calculated value for F_r/A , F_θ/A and $|F|$, and average and standard-deviation

ORIGINAL PAGE IS
OF POOR QUALITY

SEAL TEST SECTION

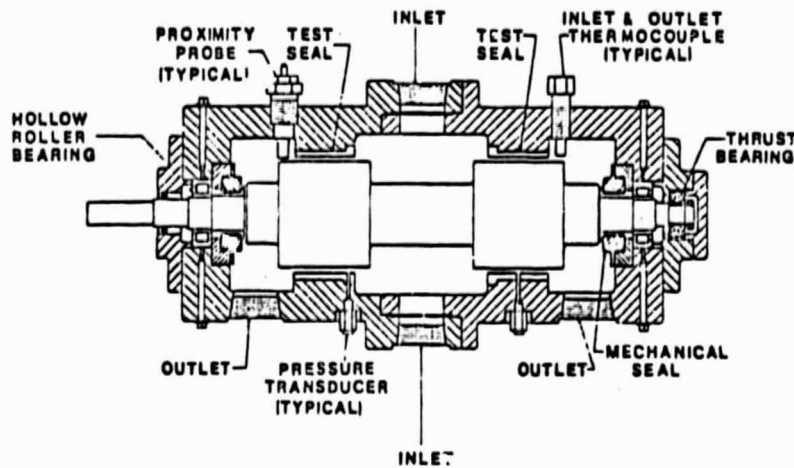


Figure 1.

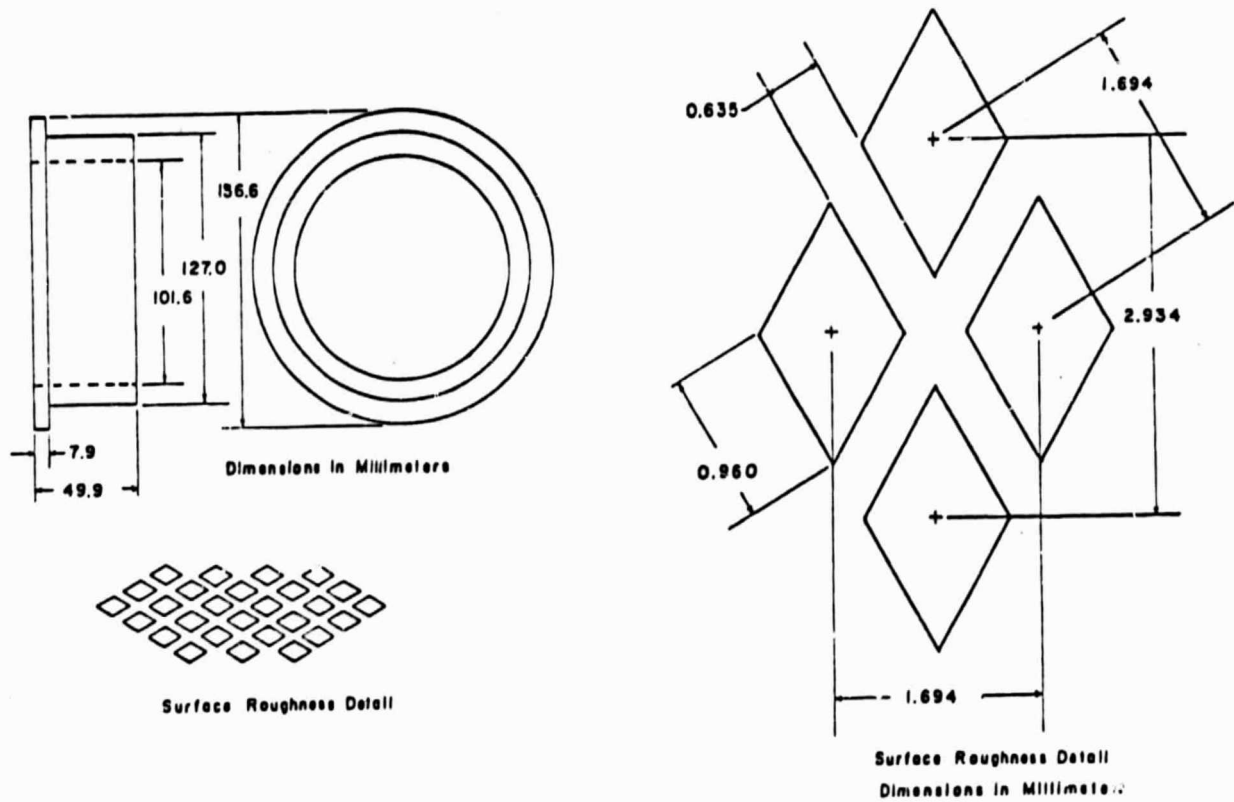


Figure 2 Rocketdyne-manufactured, knurled-indentation stator insert.

ORIGINAL PAGE IS
OF POOR QUALITY

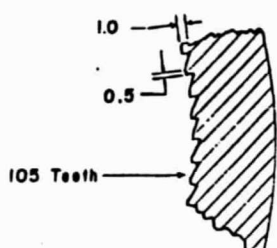
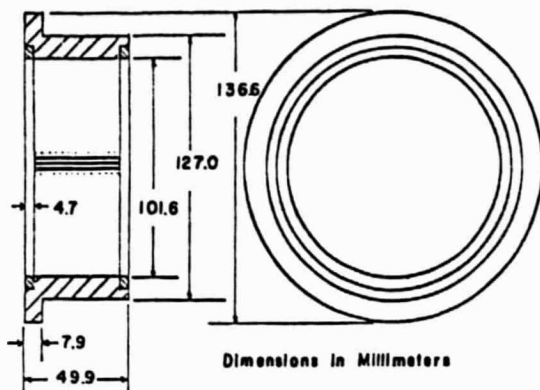


Figure 3. Axially-grooved stator insert with end seals.

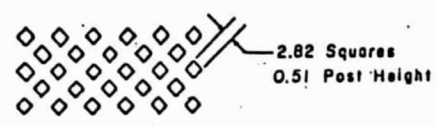
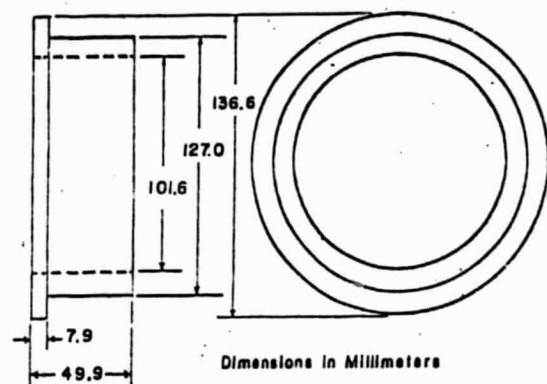


Figure 4. Diamond-grid stator insert.

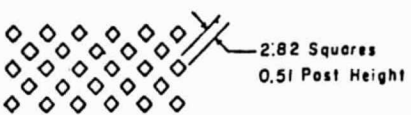
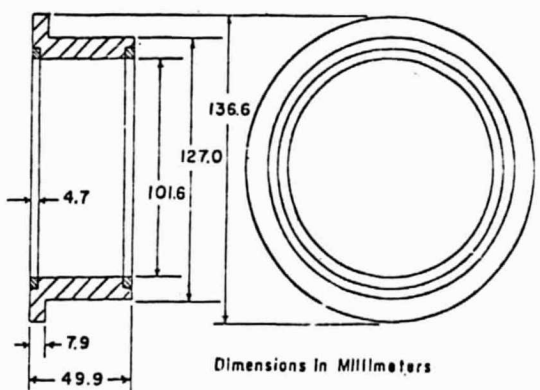


Figure 5. Diamond-grid stator insert with end seals

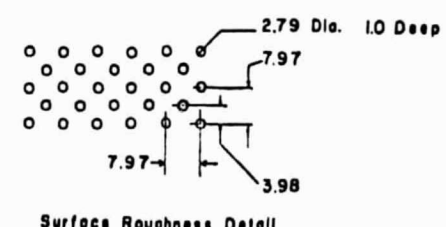
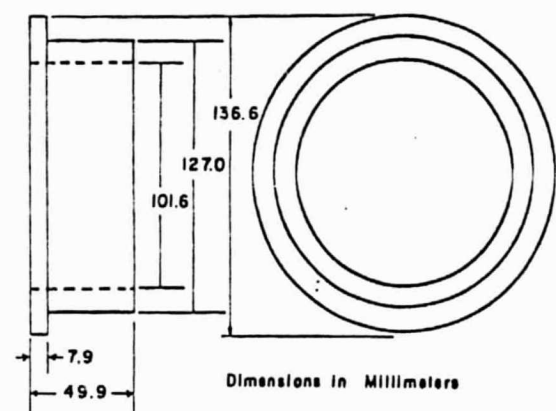


Figure 6. Round-hole pattern stator insert.

values are calculated for the test case. Observe from Eq. (3) that the test apparatus yields only the net radial and tangential force coefficients and can not be used to separately identify the seal coefficients.

The analysis of von Pragenau [4] and Childs [5] indicates that the seal rotor and stator roughness are important in defining the cross-coupled stiffness coefficient k and net-damping-force coefficient F_θ/A . Estimates for the relative roughness parameters can be obtained from measured results for the axial pressure gradient and leakage rate. The required data, consisting of the supply and discharge pressures and pressure measurements at axial locations throughout the seal, are sampled, averaged, and recorded immediately before transient data are recorded.

Test Results

For a given seal configuration, a test matrix is carried out with variations in the flowrate (axial Reynolds number) and shaft rotational speed. The flowrate is varied from a minimum value which is sufficient to yield adequate signal-to-noise ratios on the transient pressure measurement out to the maximum flow capability of the circuit. Shaft rotation speed is incremented from approximately 1,000 rpm to 7,200 rpm. In a given test series, the axial Reynolds number is held constant and the running speed incremented.

For a given test, the following two types of data are secured:

- (a) steady-state "input" data consisting of the pressure differential, average fluid density and viscosity [6], mass leakage rate, and rotational speed, and
- (b) "output" data consisting of F_r/A , F_θ/A , $|F|$ versus the axial Reynolds number and shaft running speed.

The tables of Appendices B and C provide this type of data for each test of each seal configuration.

DISCUSSION OF RESULTS: COMPARISON TO THEORY

Introduction

The theory of Appendix A does not account for either end seals or for the type of directionally-inhomogeneous roughness which is featured in the axially-grooved seal. However, it should be adequate as a model for the remaining seals. The adequacy of the theory, as determined by comparison to applicable experimental results, is the subject of this section.

Empirical Turbulence Coefficients

The theory of Appendix A characterizes the roughness of the stator and rotor by the empirical turbulence coefficients m_r , n_r (rotor) and m_s , n_s (stator) in basically the same procedure used by Yamada [7] and Hirs [8]. The theory requires estimates for these parameters based on the axial pressure gradient and leakage/axial Reynolds number data. Identification of this data was accomplished as follows.

Of the two seal inserts illustrated in figure 1, the seal on the left-hand side used the smooth seal insert, while the remaining seal inserts, were tested in the right-hand-side housing. To the extent possible, the same "very-smooth" finish was provided for both the smooth-seal insert and the rotor. The pressure gradient was measured for both the smooth and damper seals during all dynamic tests. The axial pressure gradient equation has the form

$$-\frac{\partial p}{\partial z} = \sigma \left(\frac{\rho V^2}{2} \right)$$

Hence, with a measured pressure gradient, and a known density ρ and axial velocity V , one can calculate the parameter σ , which is related to the friction-factor coefficient by

$$\sigma = \lambda \left(\frac{L}{C} \right)$$

The smooth-rotor/smooth-stator data were used to calculate values σ_r and λ_r which were assumed to apply for both the rotor and the smooth stator. From the λ_r versus running-speed, ω , and axial Reynolds, R_a , data, the empirical coefficients mr , nr of the following friction-factor formula are calculated

$$\lambda_r = nr R_a^{\frac{mr}{2}} [1 + (R\omega/V)^2]^{\frac{mr+1}{2}} \quad (4)$$

These coefficients are calculated on a least-square-error basis, and for the .394 mm (.015 in) clearance tests were as determined follows

$$nr = 0.06736, \quad mr = -0.21663 \quad (5)$$

These values can be compared to

$$no = 0.079, \quad mo = -0.25$$

from Yamada's data for "smooth" annuli.

For the smooth-rotor/damper-stator combinations, a combined σ_c is measured, which is related to the corresponding rotor σ_r and (rough) stator σ_s by

$$\sigma_c = \frac{\sigma_r + \sigma_s}{2}$$

Hence

$$\sigma_s = 2\sigma_c - \sigma_r$$

This formula was used to calculate σ_s for the damper stators by using measured values for σ_c and calculating a value for σ_r from Eq. (4) with the parameters of Eq. (5). The resultant emperical coefficients for the damper-seal stators are given in table 1. The results are generally consistent with expectations, except for the positive ms value for the round-hole-pattern stator. The data actually show an increase in σ with increasing R_a and support this result.

Colebrook's formula [9] was developed to correlate pipe-friction-factor

ORIGINAL PAGE IS
OF POOR QUALITY

	Emperical Coefficients		Relative Roughness
	ms	ns	$\epsilon = e/2C$
Smooth $C_r = .394 \text{ mm}$	-.21663	.06736	.0003866
Smooth $C_r = .527 \text{ mm}$	-.23980	.09885	.0006919
Rocketdyne $C_r = .527 \text{ mm}$	-.13567	.06968	.022
Diamond-Grid $C_r = .527 \text{ mm}$	-.03498	.11815	.45973
Hole Pattern $C_r = .527 \text{ mm}$.01904	.015027	.05752

Table 1. Emperical turbulence coefficients ms, ns for damper seal configurations, and estimates for relative-roughness from Colebrook's formula [9] at $R_a = 300,000$.

$\epsilon = e/2C$	mo	no
10^{-8}	-.19893	.04506
10^{-7}	-.19873	.04494
10^{-6}	-.19804	.04460
10^{-5}	-.19309	.04228
10^{-4}	-.15745	.02895
10^{-3}	-.07146	.01308
10^{-2}	-.01567	.01170
10^{-1}	-.00242	.02622
1	-.00060	.19434

Table 2. Emperical turbulence coefficients mo, no as calculated from Colebrook's formula [9].

data as a function of axial Reynolds number $\bar{R}_a = VD/\gamma$ and relative roughness $\epsilon = e/D$. If Colebrook's formula is used to calculate a friction factor for flow in an annulus (with the same roughness on both surfaces) versus $R_a = 2VC/v$, then the empirical coefficients of table 2 result. Estimates of the relative and absolute roughness range for a stator can be obtained from this table by entering with estimates of m_s , n_s from test results and then "looking up" the corresponding estimates for relative roughness. The fact that λ , as defined by Eq. (4), is a weak function of ω at high values of R_a generally supports this procedure. Table 1 provides estimates for the relative roughness of the stator elements based on Colebrook's formula.

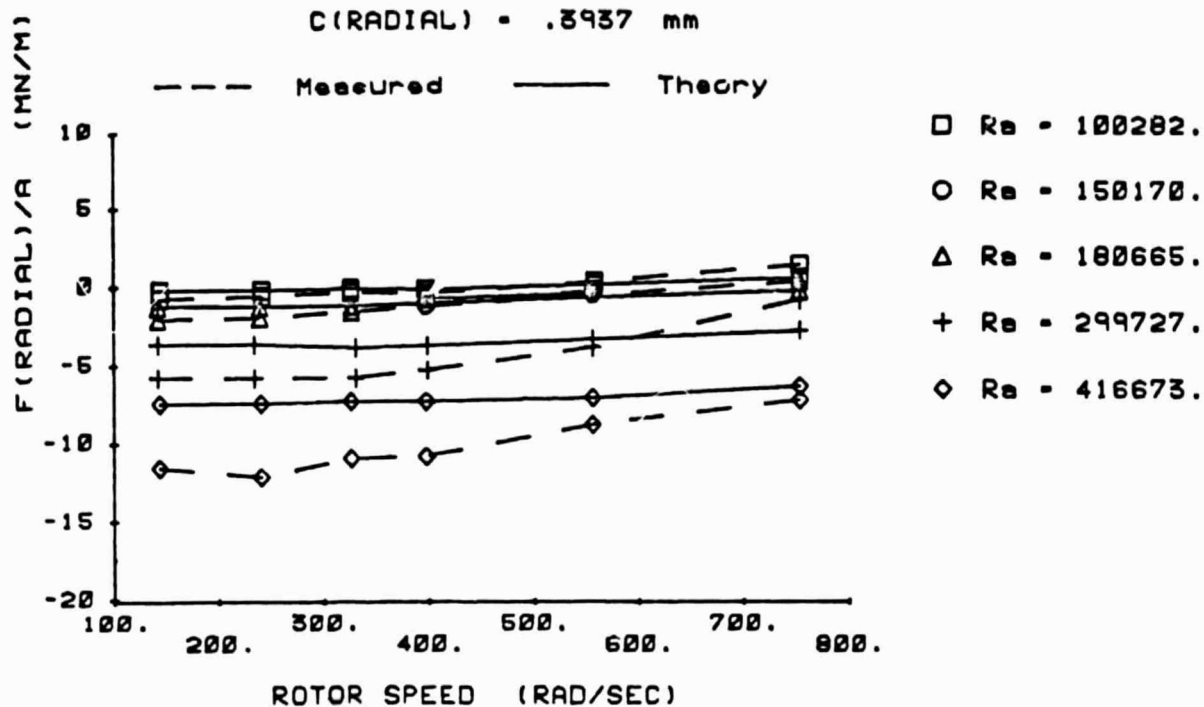
Dynamic Test Data

Figure 7 illustrates measured and theoretical results for F_r/A and F_θ/A versus R_a and ω for the smooth stator with $C_r = .394$ mm. The measured results are taken from table C.1, while the theoretical results are calculated using the analysis of Appendix A with the emperical parameters of table 2. An inspection of these results demonstrates a "reasonable" agreement between theory and experiment with respect to the tangential force but much large measured radial-force-coefficient magnitudes at low speeds than predicted. Further, the magnitude of F_r/A decreases more rapidly with increasing running speed than predicted. Figures 8 through 14 illustrate measured and, where appropriate, theoretical predictions for the remaining seals which were tested.

Eq. (3) provides the basis for a quantitative comparison of theory and experiment. At first glance these equations suggest that sufficient independent equations could be obtained to calculate all the rotordynamic coefficients by simply testing at three running speeds. However, the fact that the coefficients depend on ω precludes this approach. While K , C , and M are weak functions of ω through their dependence on σ , the "cross-coupled"

FINITE-LENGTH THEORY
SMOOTH STATOR / SMOOTH ROTOR
 $C(\text{RADIAL}) = .3937 \text{ mm}$

ORIGINAL PAGE IS
OF POOR QUALITY



FINITE-LENGTH THEORY
SMOOTH STATOR / SMOOTH ROTOR
 $C(\text{RADIAL}) = .3937 \text{ mm}$

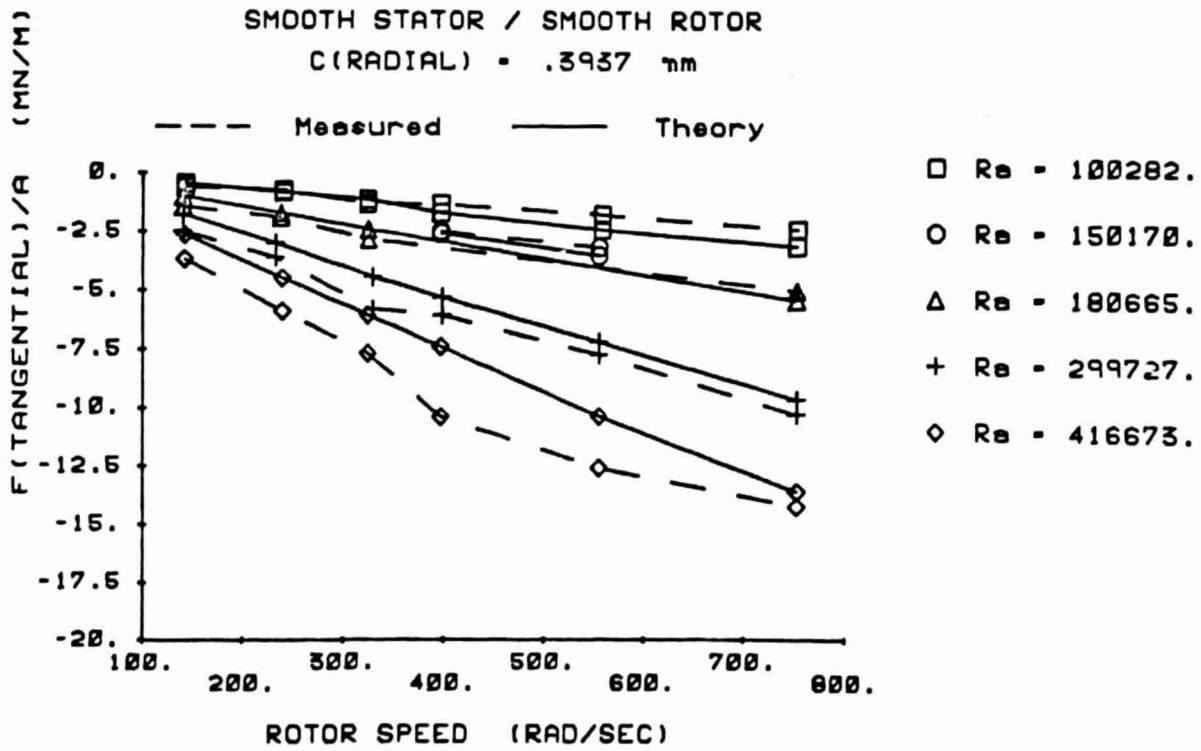


Figure 7. Measured and finite-length [5] theoretical results for F_r/A and F_θ/A ; smooth stator, $C_r = .394 \text{ mm}$.

ORIGINAL PAGE IS
OF POOR QUALITY

FINITE-LENGTH THEORY
ROCKETDYNE STATOR / SMOOTH ROTOR
 $C(\text{RADIAL}) = .3937 \text{ mm}$

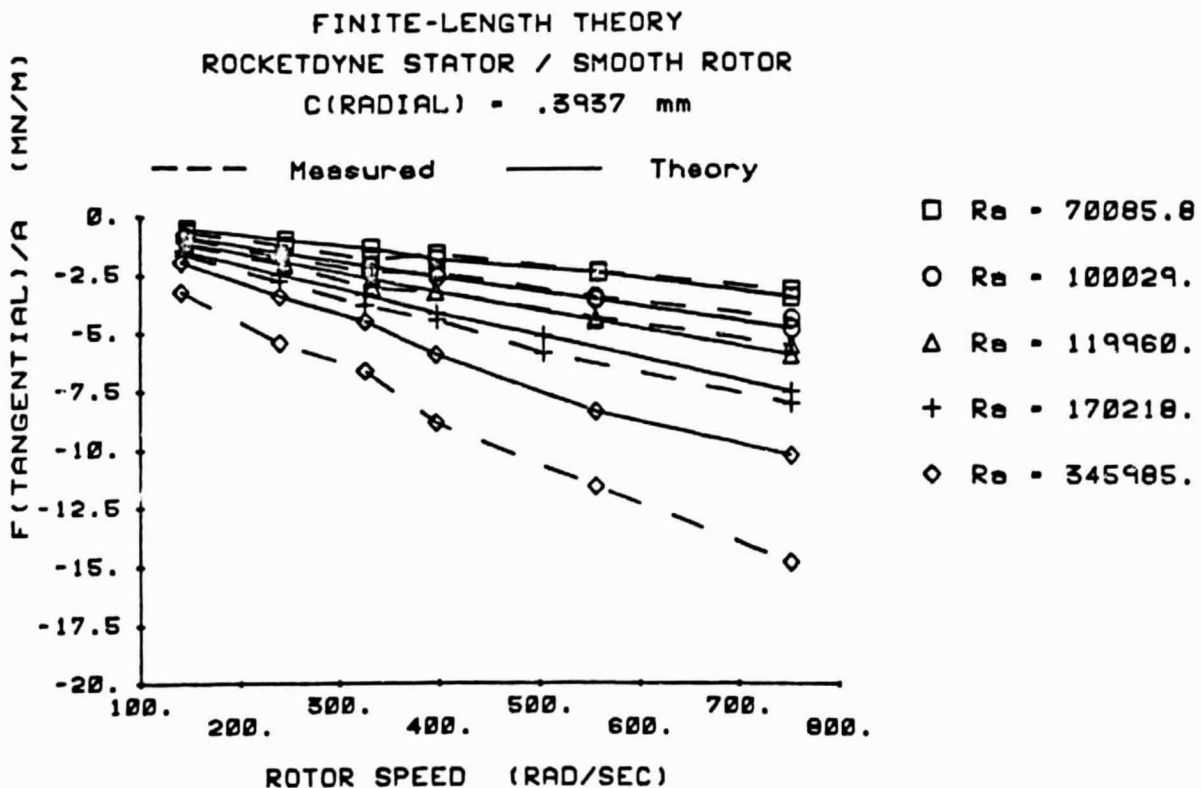
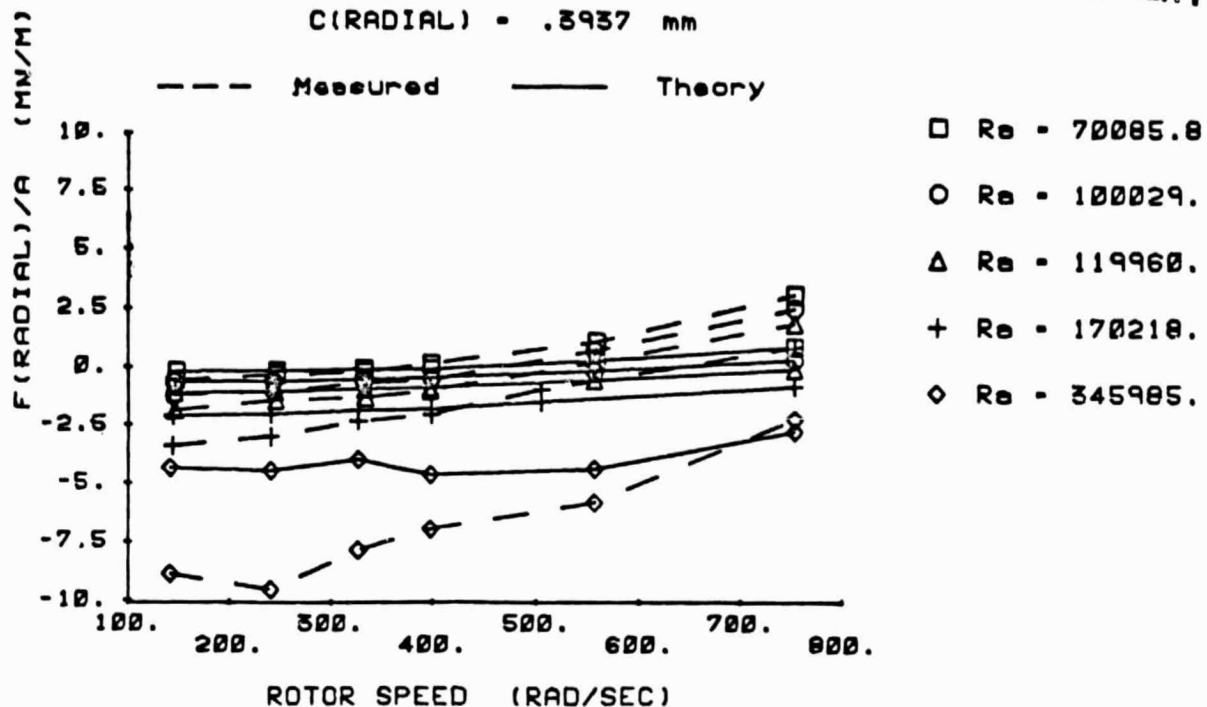


Figure 8. Measured and finite-length [5] theoretical results for F_r/A and F_θ/A ; Rocketdyne stator, $C_r = .394 \text{ mm}$.

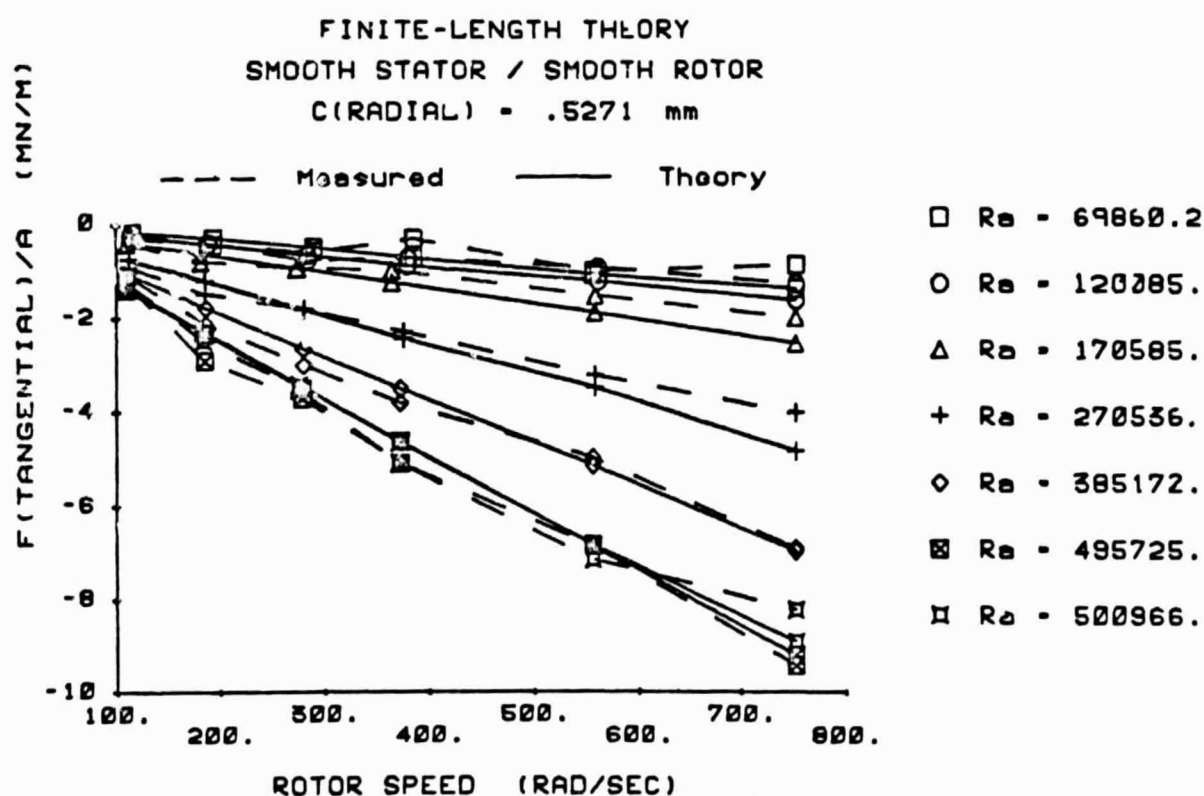
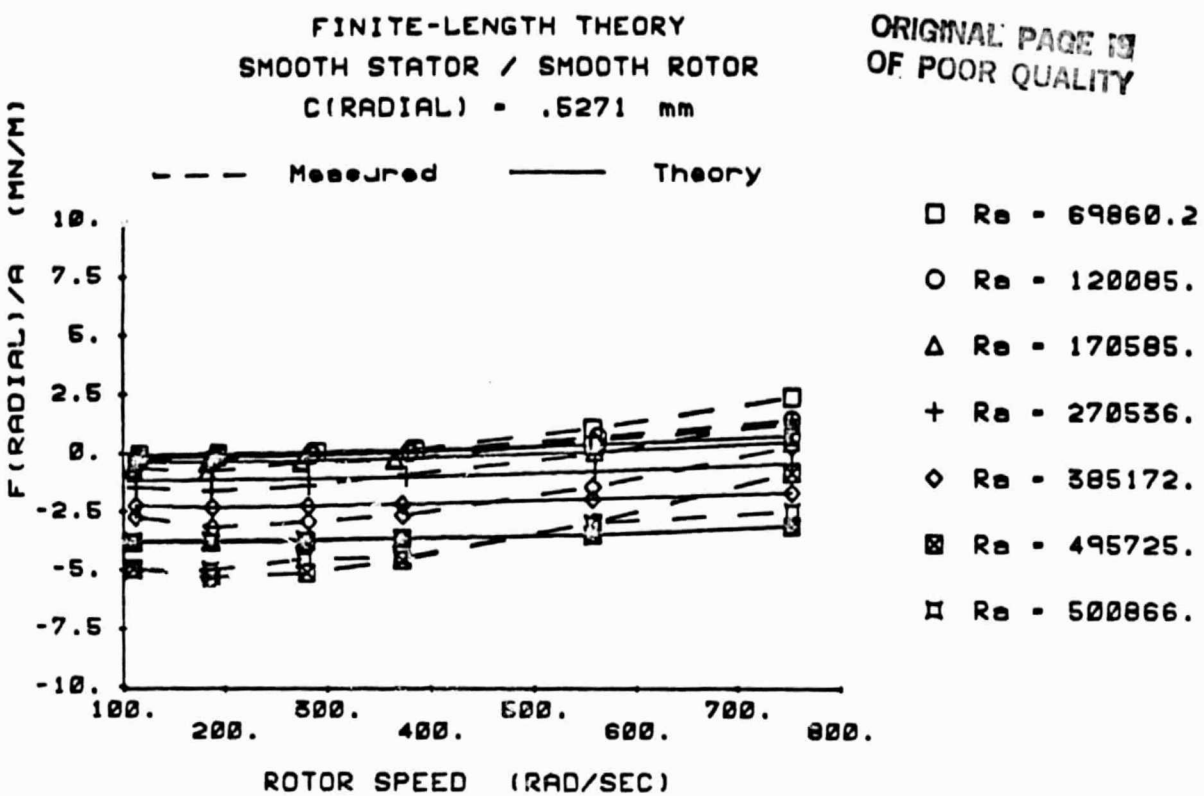


Figure 9. Measured and finite-length [5] theoretical results for F_r/A and F_θ/A ; smooth stator, $C_r = .527 \text{ mm}$.

FINITE-LENGTH THEORY
ROCKETDYNE STATOR / SMOOTH ROTOR
 $C(\text{RADIAL}) = .5271 \text{ mm}$

ORIGINAL PAGE IS
OF POOR QUALITY

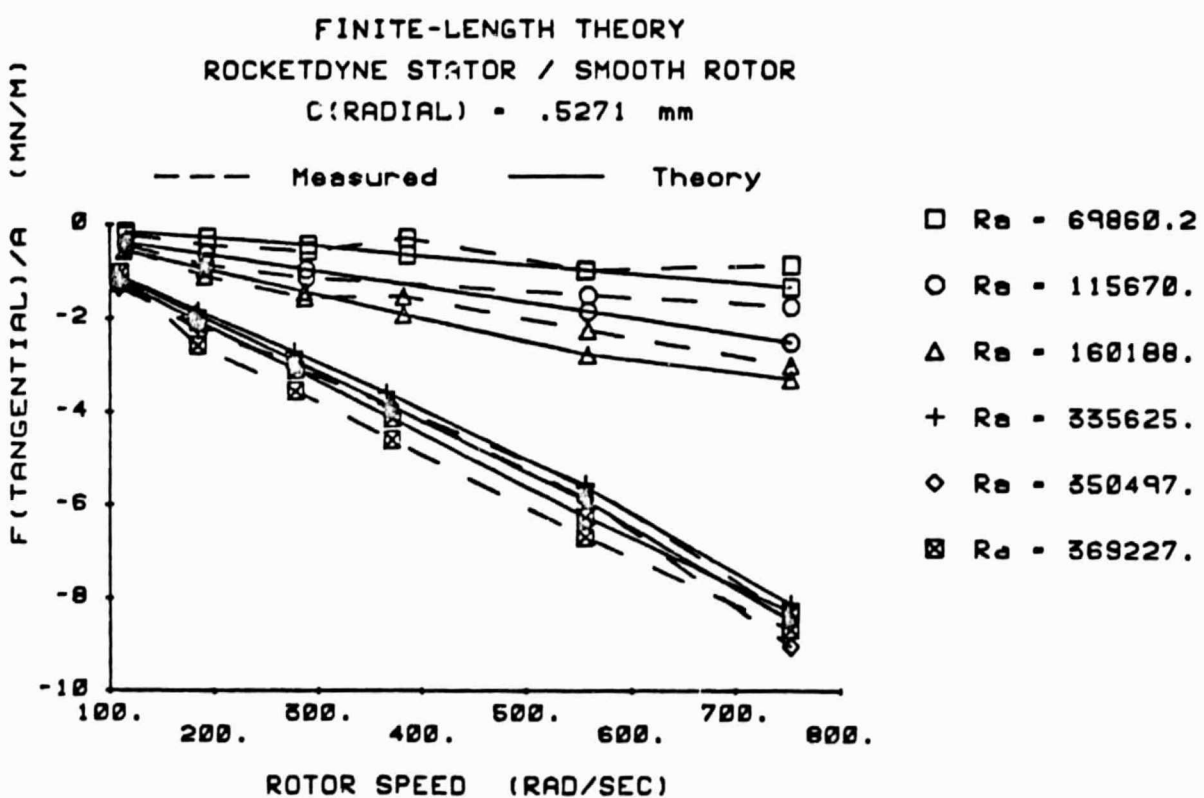
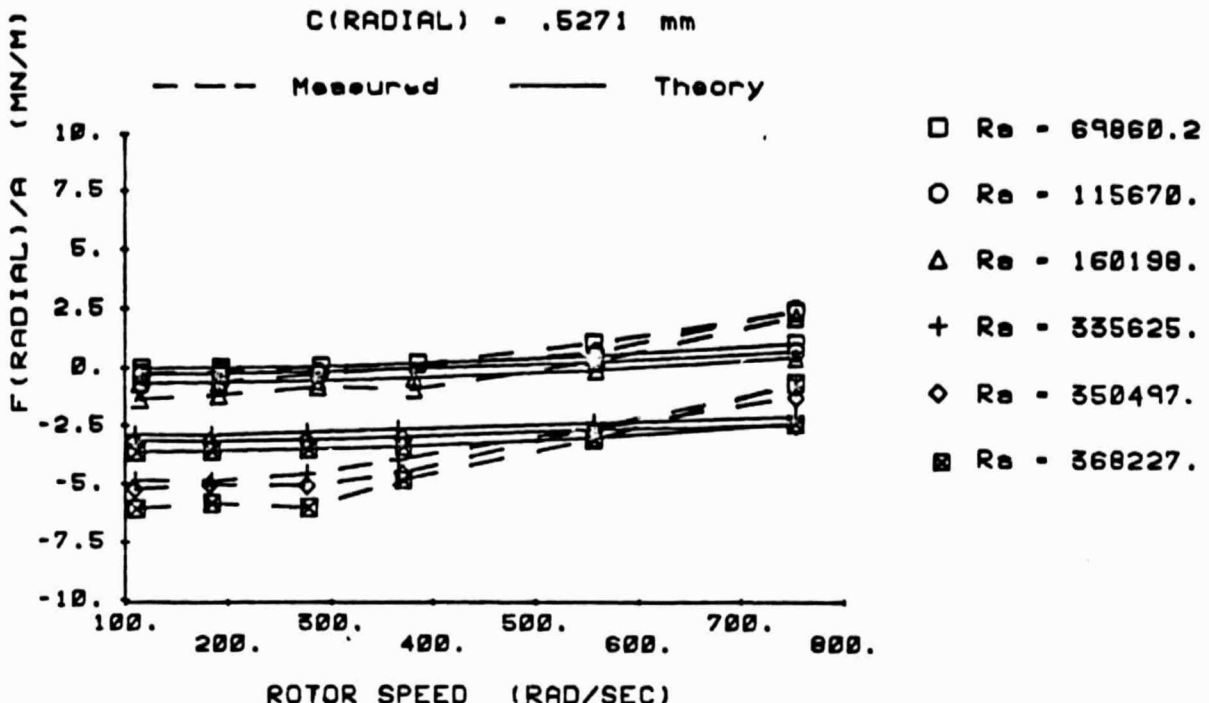


Figure 10. Measured and finite-length [5] theoretical results for F_r/A and F_θ/A ; Rocketdyne-knurled stator; $C_r = .527 \text{ mm}$.

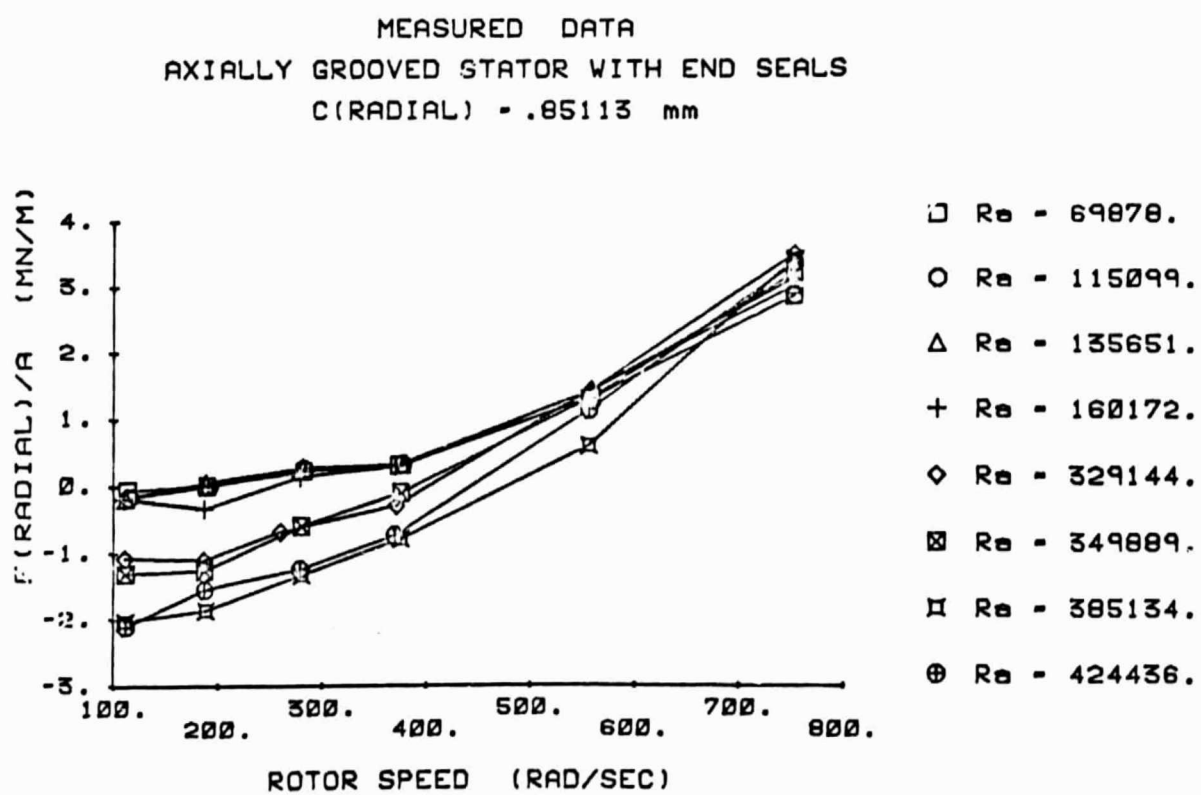
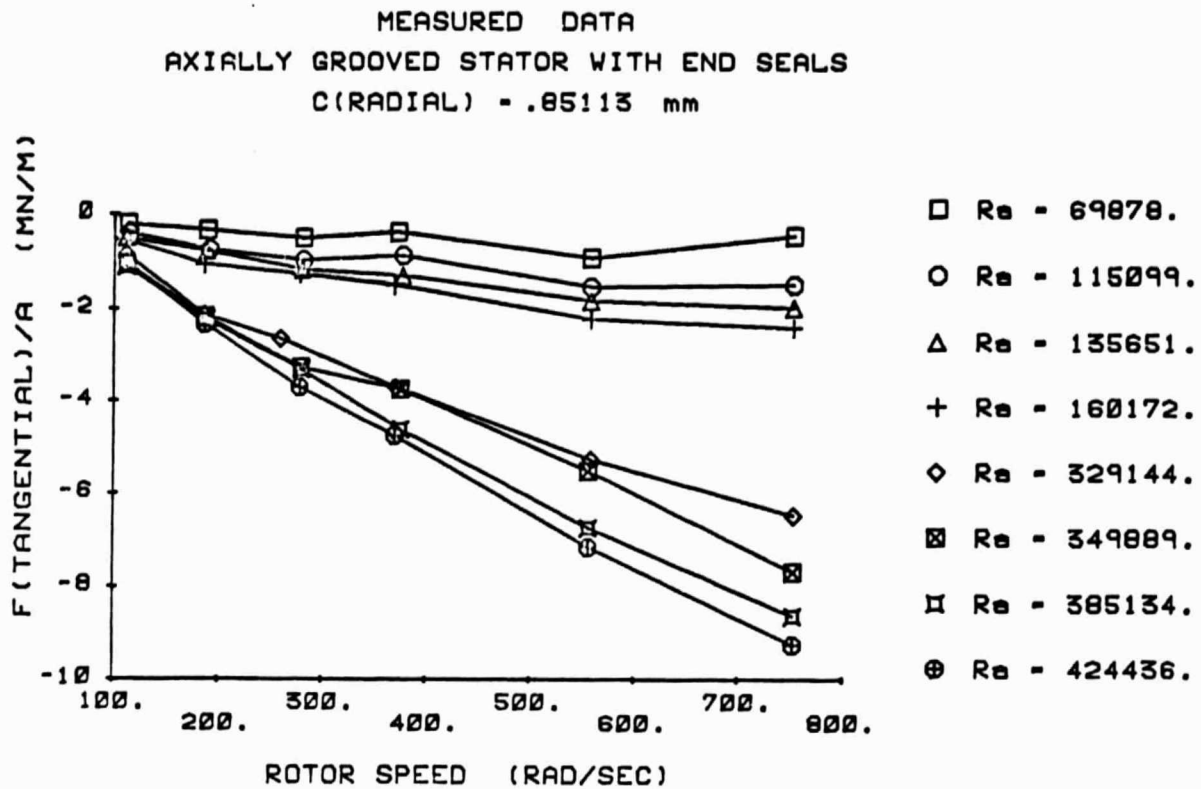
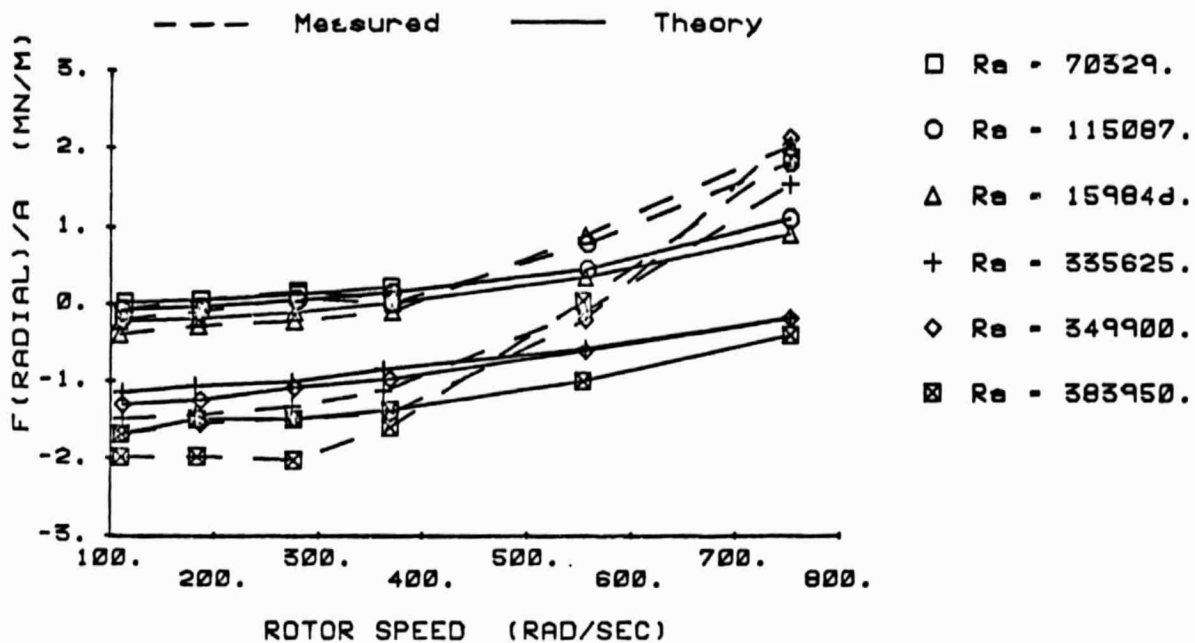


Figure 11. Measured results for F_r/A and F_θ/A ; axially-grooved stator with end seals.

ORIGINAL PAGE IS
OF POOR QUALITY

FINITE-LENGTH THEORY
DIAMOND GRID STATOR / SMOOTH ROTOR
 C (RADIAL-AVERAGE) = .889 mm



FINITE-LENGTH THEORY
DIAMOND GRID STATOR / SMOOTH ROTOR
 C (RADIAL-AVERAGE) = .889 mm

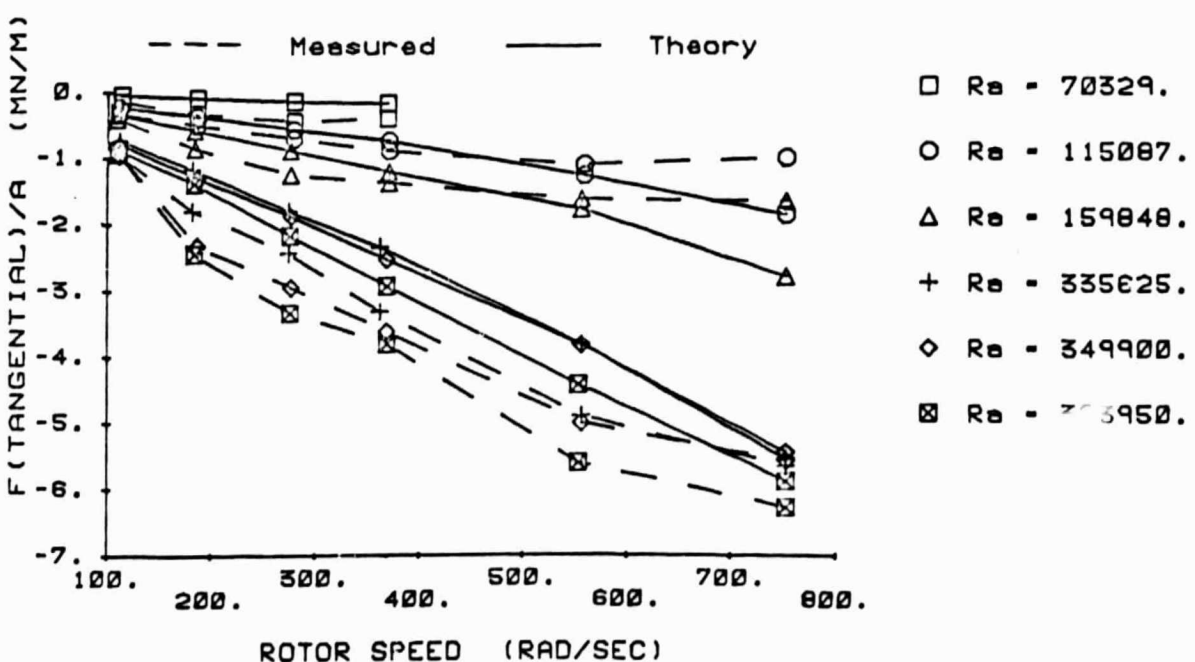
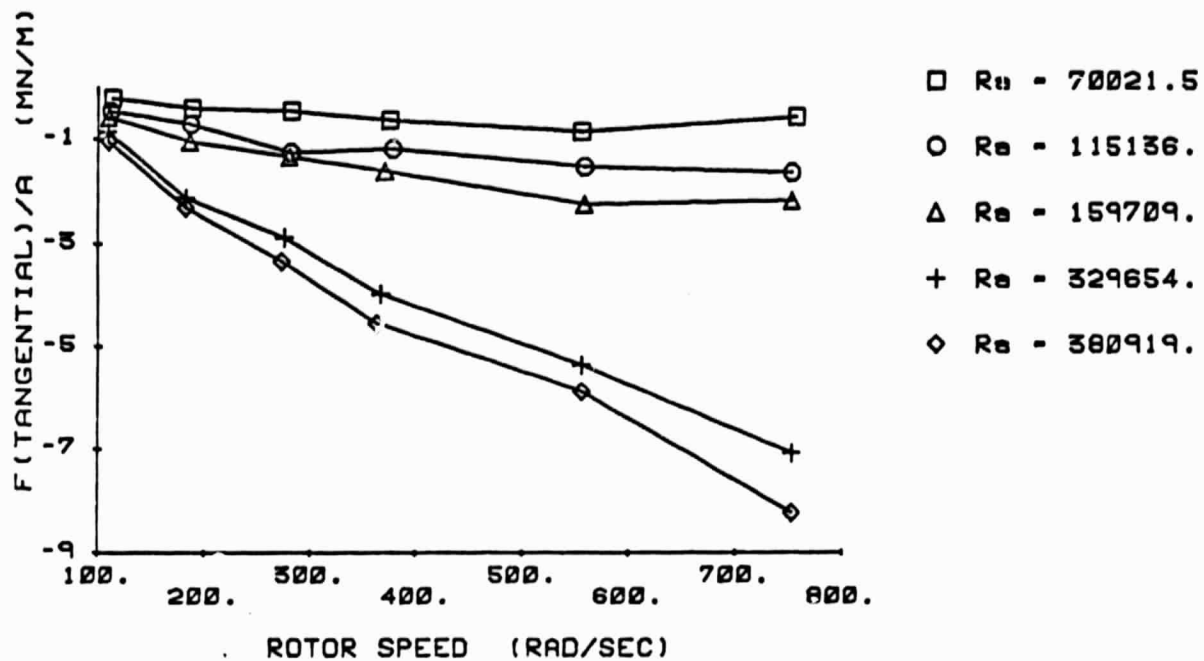


Figure 12. Measured and finite-length [5] theoretical results for F_r/A and F_θ/A ; diamond-grid stator.

MEASURED DATA
DIAMOND GRID STATOR WITH END SEALS
 $C(\text{RADIAL}) = .8163 \text{ mm}$



MEASURED DATA
DIAMOND GRID STATOR WITH END SEALS
 $C(\text{RADIAL}) = .8163 \text{ mm}$

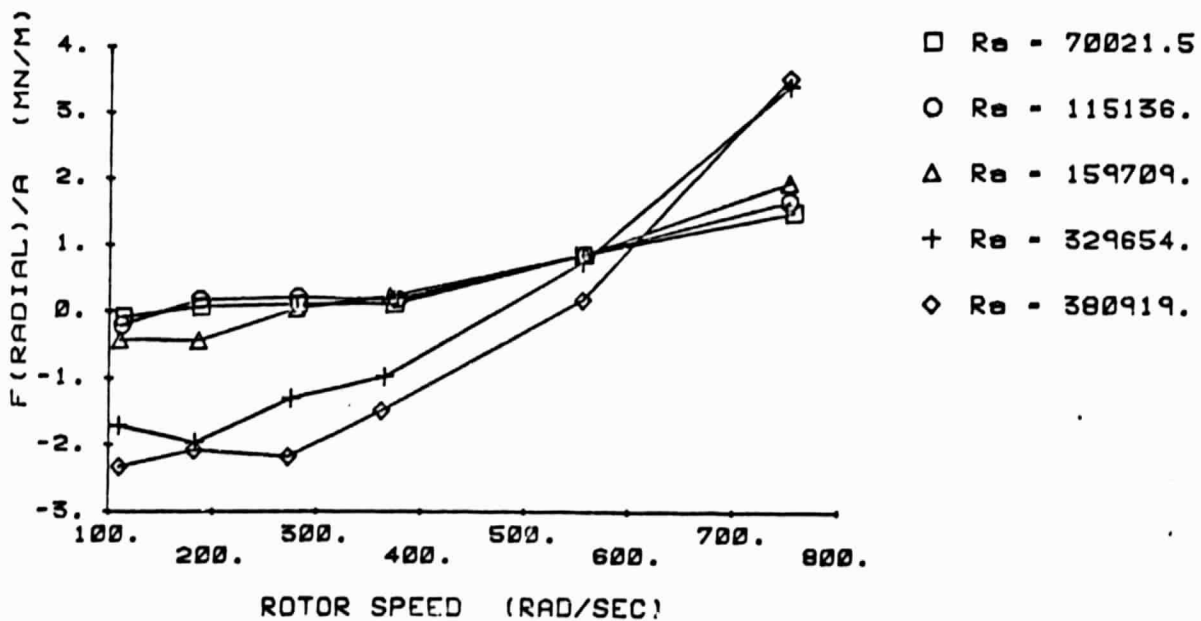
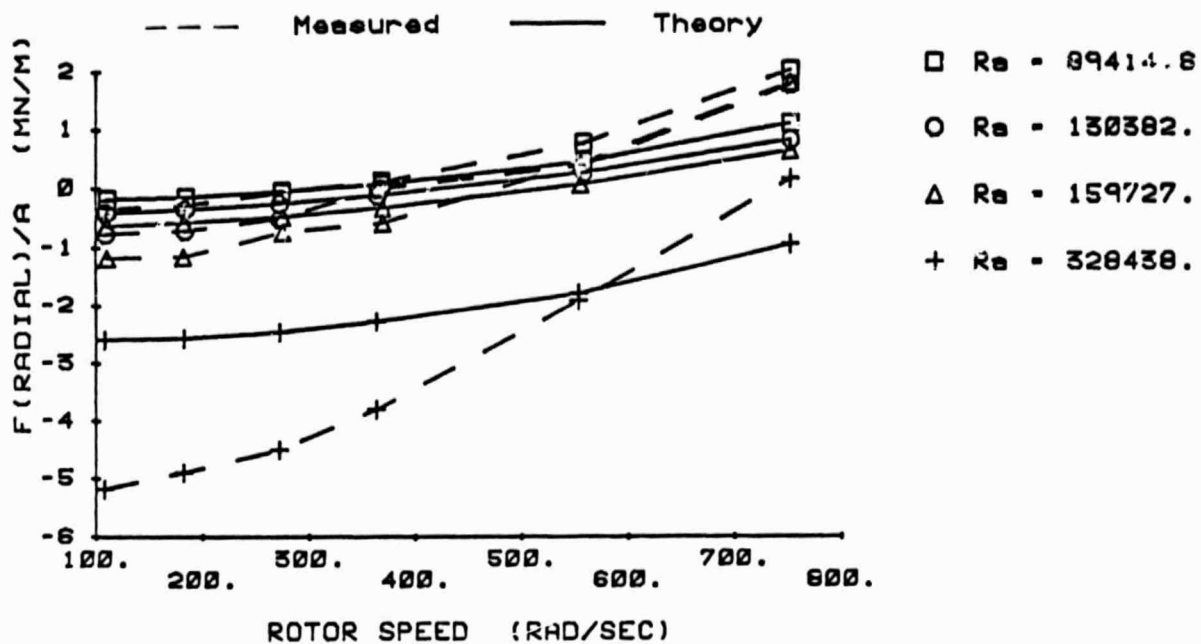


Figure 13. Measured results for F_r/A and F_θ/A ; diamond-grid with end seals.

FINITE-LENGTH THEORY
ROUGH STATOR : HOLE PATTERN 1



FINITE-LENGTH THEORY
ROUGH STATOR : HOLE PATTERN 1

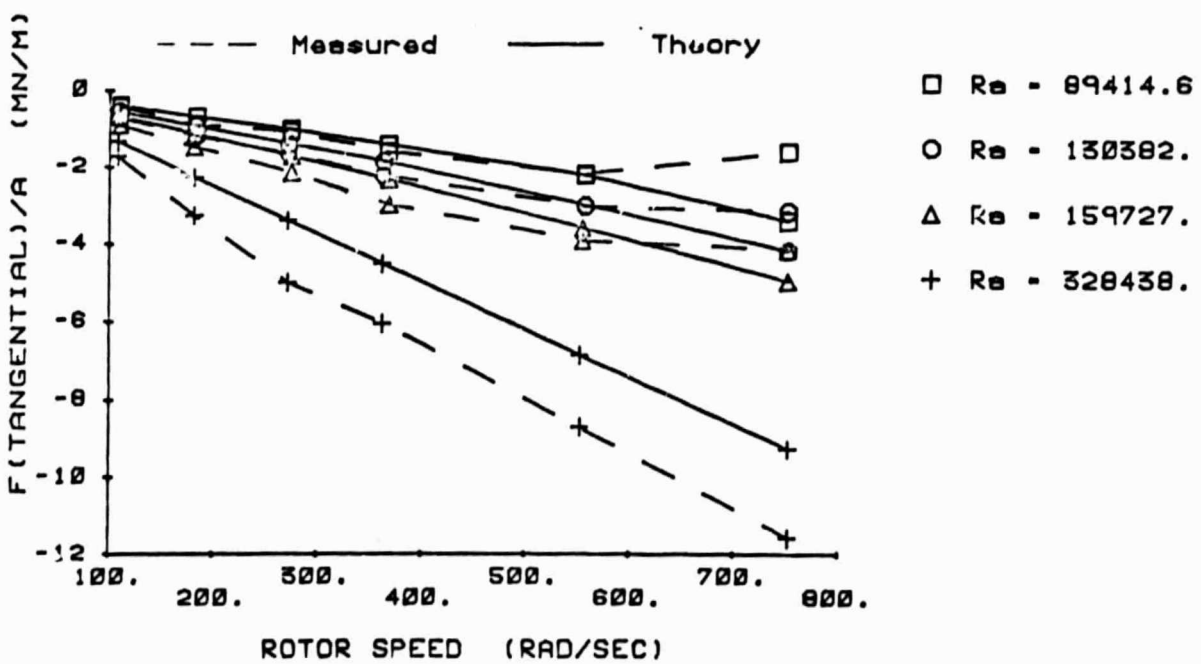


Figure 14. Measured and finite-length [5] theoretical results for F_r/A and F_θ/A ; round hold-hole pattern stator.

coefficients k and c are linear functions of ω . In fact, if the fluid is prerotated prior to entering the seal such that the inlet tangential velocity is $U_{\theta 0} = R\omega/2$, then theory predicts that $k = C\omega/2$, $c = M\omega$, and

$$F_r/A = -K, \quad F_\theta/A = -C\omega/2 \quad (6)$$

The present test apparatus provides no intentional prerotation, and the expected result is of the form

$$\begin{aligned} k &= b_1 C\omega/2, \quad b_1 < 1 \\ c &= b_2 M\omega, \quad b_2 < 1 \end{aligned} \quad (7)$$

$$\begin{aligned} F_\theta/A &\cong -C_{ef}\omega = -C(1-b_1/2)\omega \\ F_r/A &\cong -K_{ef} + M_{ef}\omega^2 = -K + M(1 - b_2)\omega^2 \end{aligned} \quad (8)$$

The term C_{ef} denotes the "net damping coefficient" resulting from the drag force $C\omega A$ and the forward whirl excitation force kA . A direct comparison between theory and experiment is obtained by curvefitting the theoretical and experimental results for the F_r/A and F_θ/A to obtain predictions for K_{ef} , C_{ef} , and M_{ef} . Note that the procedure of curvefitting the data with respect to ω eliminates the running-speed dependency. Further, K_{ef} is the zero-running speed intercept of the F_r/A versus ω curve, and C_{ef} is the slope of the F_θ/A versus ω curve.

A comparison of the curve-fitted results are provided in table 3 for the smooth and Rocketdyne-knurled seal for the two clearance values $C_r = .394$ and $.527$ mm. The results support the following general conclusions:

- (a) Theoretical direct stiffness values are smaller than predicted, and the discrepancy increases with decreasing clearances.
- (b) Theoretical predictions of C_{ef} are generally in good agreement with test results. The agreement generally improves with increasing R_a .

**ORIGINAL PAGE IS
OF POOR QUALITY**

FINITE LENGTH THEORY
S. I. Units:

	KEF(EXP)	KEF(THEORY)	CEF(EXP)	CEF(THEORY)	MEF(EXP)	MEF(THEORY)	KEF(EX/TH)	CEF(EX/TH)	MEF(EX/TH)
ROCKETDYNE STATOR / SMOOTH ROTOR									
RA= 0.7009E 05	0.3517E 06	0.9266E 05	C(RADIAL) = .3937 mm				3.410	3.796	0.8082
RA= 0.1000E 06	0.1212E 07	0.6455E 06	3891.	4814.	8.457	2.419	1.878	0.8515	2.49
RA= 0.1200E 06	0.1947E 07	0.1186E 07	5329.	6493.	7.199	2.067	1.641	0.8777	3.48
RA= 0.1702E 06	0.4195E 07	0.2176E 07	6999.	7975.	2.834	2.151	1.910	1.065	1.31
RA= 0.3460E 06	0.9441E 07	0.3525E 07	0.1059E 05	9944.	0.1402E 05	12.76	9.213	2.678	1.364
SMOOTH STATOR / SMOOTH ROTOR									
RA= 0.1003E 06	0.6717E 06	0.1547E 06	C(RADIAL) = .3937 mm				5.029	2.402	4.342
RA= 0.1502E 06	0.1349E 07	0.1015E 07	3023.	4621.	8.258	2.528	1.329	0.7184	2.09
RA= 0.1807E 06	0.2300E 07	0.1131E 07	4332.	6031.	3.140	3.092	2.034	0.8173	3.26
RA= 0.2997E 06	0.4998E 07	0.3321E 07	5943.	7272.	0.1255E 05	0.1290E 05	4.637	1.305	1.01
RA= 0.4167E 06	0.1224E 08	0.7216E 07	0.1782E 05	0.1809E 05	7.759	3.550	1.696	0.9849	3.82
ROCKETDYNE STATOR / SMOOTH ROTOR									
RA= 0.6986E 05	0.1281E 06	0.1663E 05	C(RADIAL) = .5271 mm				6.420	2.370	7.698
RA= 0.1157E 06	0.5565E 06	0.3413E 06	1076.	1920.	7.521	1.772	1.630	0.5613	2.70
RA= 0.1602E 06	0.1108E 07	0.6937E 06	1885.	3358.	8.792	2.301	1.598	0.8166	4.24
RA= 0.3356E 06	0.5121E 07	0.3052E 07	3619.	4431.	0.1067E 05	0.1085E 05	0.3798	1.678	3.82
RA= 0.3505E 06	0.5469E 07	0.3286E 07	0.1060E 05	0.1130E 05	7.090	0.6284	1.664	0.9836	18.6
RA= 0.3682E 06	0.6189E 07	0.3628E 07	0.1131E 05	0.1106E 05	11.00	2.599	1.706	1.027	11.2
SMOOTH STATOR / SMOOTH ROTOR									
RA= 0.6986E 05	0.1281E 06	0.5139E 05	C(RADIAL) = .5271 mm				6.420	1.627	2.492
RA= 0.1201E 06	0.3097E 06	0.2336E 06	1076.	1975.	1423.	2.294	1.651	2.182	0.5448
RA= 0.1706E 06	0.9087E 06	0.4100E 06	2328.	3373.	2.333	1.831	2.216	0.6636	1.38
RA= 0.2705E 06	0.1516E 07	0.1169E 07	4810.	6357.	6.854	1.539	1.297	0.6900	1.38
RA= 0.3852E 06	0.2575E 07	0.2254E 07	8613.	9212.	10.57	1.536	1.142	0.7567	4.45
RA= 0.4957E 06	0.4842E 07	0.3841E 07	0.1210E 05	0.1215E 05	12.47	1.333	1.261	0.9350	6.89
RA= 0.5009E 06	0.5494E 07	0.3717E 07	0.1111E 05	0.1182E 05	1.666	1.689	1.478	0.9401	9.35
									0.986

Table 3. K_{ef} , C_{ef} , and M_{ef} coefficients from measured and theoretical results;
smooth and Rocketdyne-knurled stators for $C_r = .394$ and .527 mm.

- (c) Measured values for M_{ef} are substantially larger than predictions.

This result is at odds with earlier test results for constant-clearance and convergent-tapered seals which were tested in water [10].

Table 4 contains the corresponding results for all of the seals tested with the minimum clearance C_r (min) = .527 mm. A review of the additional results for the diamond-grid and round-hole-pattern-roughness stator supports the following conclusions:

Diamond-Grid Stator

- (a) Theoretical direct stiffness values are smaller than predicted, but the agreement is the best of all seals tested.
- (b) Measured C_{ef} values are smaller than predicted at lower values of R_a but are well predicted at higher values.
- (c) Theory underpredicts M_{ef} .

Round-Hole-Pattern Stator

- (a) Measured direct stiffness values are much higher than predicted, and the discrepancy worsens as R_a increases. At high values of R_a , the discrepancy between theory and experiment is worse for this seal than any seal tested.
- (b) C_{ef} is overestimated at low values of R_a and underestimated at high values.
- (c) Theory underpredicts M_{ef} .

**ORIGINAL PAGE IS
OF POOR QUALITY**

S. I. Units

KEF (EXP)	KEF (THEORY)	CEF (EXP)	CEF (THEORY)	MEF (EXP)	MEF (THEORY)	MEF (EXP)	MEF (THEORY)	KEF (EXP/TH)	CEF (EXP/TH)	MEF (EXP/TH)	MEF (THEORY)
ROCKETDYNE STATOR / SMOOTH ROTOR											
RA= 0.6986E 05	0.1281E 06	0.1663E 05	1076.	1920.	6.420	2.370	7.698	0.5603	2.70	0.5603	2.70
RA= 0.1157E 06	0.5565E 06	0.4131E 06	1885.	3358.	7.521	1.772	1.630	0.5613	4.24	0.5613	4.24
RA= 0.1602E 06	0.1108E 07	0.6937E 06	3619.	4431.	8.792	2.301	1.598	0.8166	3.82	0.8166	3.82
RA= 0.3356E 05	0.5121E 07	0.3052E 07	0.1067E 05	0.1085E 05	7.064	0.3798	1.678	0.9836	18.6	0.9836	18.6
RA= 0.3505E 06	0.5469E 07	0.3286E 07	0.1160E 05	0.1130E 05	7.070	0.6284	1.664	1.027	11.2	1.027	11.2
RA= 0.3682E 06	0.6189E 07	0.3628E 07	0.1151E 05	0.1106E 05	11.00	2.599	1.706	1.041	4.23	1.041	4.23
SMOOTH STATOR / SMOOTH ROTOR											
RA= 0.6986E 05	0.1281E 06	0.5133E 05	1076.	1975.	6.420	1.627	2.492	0.5448	3.94	0.5448	3.94
RA= 0.1201E 06	0.5097E 06	0.2336E 06	1423.	2144.	2.294	1.651	2.182	0.6636	1.38	0.6636	1.38
RA= 0.1706E 06	0.9087E 06	0.4100E 06	2328.	3373.	2.533	1.831	2.216	0.6900	1.38	0.6900	1.38
RA= 0.2705E 06	0.1516E 07	0.1169E 07	4810.	6357.	6.854	1.539	1.297	0.7567	4.45	0.7567	4.45
RA= 0.3852E 06	0.2575E 07	0.2254E 07	8613.	9212.	10.57	1.536	1.142	0.9350	6.88	0.9350	6.88
RA= 0.4957E 06	0.4842E 07	0.3841E 07	0.1210E 05	0.1215E 05	12.47	1.333	1.261	0.9964	9.35	0.9964	9.35
RA= 0.5009E 06	0.5494E 07	0.3717E 07	0.1111E 05	0.1182E 05	1.686	1.689	1.478	0.9401	0.986	0.9401	0.986
AXIALLY GROOVED STATOR WITH END SEALS											
RA= 0.6988E 05	-0.1172E 06	610.7	1728.	610.7	7.648	7.012	7.374	7.374	1.975	1.975	1.975
RA= 0.1151E 06	0.1297E 05	3717.	2347.	2958.	7.943	8409.	9.367	9.367	1.745	1.745	1.745
RA= 0.1357E 05	0.1602E 06	0.1625E 06	RA= 0.3291E 06	0.1174E 07	8409.	9875.	6.043	6.043	2.690	2.690	2.690
RA= 0.3499E 06	0.1686E 07	0.2009E 07	RA= 0.3851E 06	0.2306E 07	0.1175E 05	10.80	0.1267E 05	7.6889	2.261	2.261	2.261
RA= 0.4244E 06	0.1865E 07	0.1653E 07	RA= 0.3844E 06	0.1826E 07	7.858.	10.53	2.179	2.179	1.310	1.310	1.310
DIAMOND GRID STATOR											
RA= 0.7033E 05	0.4976E 06	3227.	985.2	498.8	.8890 mm	-8.284	1.712	1.712	1.745	1.745	1.745
RA= 0.1151E 06	0.6021E 05	0.3451E 05	1088.	2551.	5.078	2.690	2.690	2.690	4.265	4.265	4.265
RA= 0.1598E 06	0.3052E 06	0.2330E 06	1775.	3701.	5.909	2.261	2.261	2.261	4.795	4.795	4.795
RA= 0.3356E 06	0.1301E 07	0.1221E 07	RA= 0.3499E 06	0.1142E 07	7416.	8.185	1.079	1.079	1.065	1.065	1.065
RA= 0.3297E 06	0.1699E 07	0.1424E 07	RA= 0.3844E 06	0.1826E 07	6892.	7193.	12.52	1.047	0.8026	0.8026	0.8026
RA= 0.3809E 06	0.1865E 07	0.1653E 07	RA= 0.3844E 06	0.1826E 07	7950.	7858.	10.53	2.179	1.128	1.128	1.128
DIAMOND GRID STATOR WITH END SEALS											
RA= 0.7002E 05	0.7552E 05	RA= 0.1151E 06	0.1224E 06	RA= 0.1597E 06	0.6342E 06	RA= 0.3297E 06	0.1699E 07	RA= 0.3809E 06	C (RADIAL-AVERAGE) = .81638 mm	3.159	-4.83
RA= 0.1151E 06	0.8111E 06	0.4587E 06	RA= 0.1268E 07	0.6766E 06	0.5275.	1782.	2.974	2.974	3.100	3.100	3.100
RA= 0.1597E 06	0.6342E 06	0.2582E 07	RA= 0.1826E 07	0.1061E 05	9257.	2544.	12.22	12.22	1.065	1.065	1.065
RA= 0.3284E 06	0.5616E 07	0.1234E 05	RA= 0.3844E 06	0.1826E 07	0.1486E 05	0.1234E 05	6.693	6.693	3.556	3.556	3.556
ROTOR STATOR : HOLE PATTERN 1											
RA= 0.8941E 05	0.2755E 06	0.1751E 06	RA= 0.1304E 06	0.4587E 06	RA= 0.1597E 06	RA= 0.3284E 06	0.1699E 07	RA= 0.3809E 06	C = 0.5080 mm	2.672	1.573
RA= 0.1304E 06	0.8111E 06	0.3974.	RA= 0.1268E 07	0.5680.	RA= 0.1597E 06	RA= 0.3297E 06	0.1699E 07	RA= 0.3809E 06	RA= 0.3844E 06	4.395	1.949
RA= 0.1597E 06	0.6342E 06	0.5275.	RA= 0.1826E 07	0.6705.	RA= 0.3297E 06	RA= 0.3809E 06	0.1699E 07	RA= 0.3844E 06	RA= 0.3844E 06	5.292	2.050
RA= 0.3284E 06	0.5616E 07	0.1234E 05	RA= 0.3844E 06	0.1826E 07	0.1486E 05	0.1234E 05	6.693	6.693	3.556	3.556	3.556

Table 4. KEf, Cef, and Mef coefficients from measured and (where appropriate) theoretical predictions for all seals tested which have Cr = .527 mm.

DISCUSSION OF RESULTS: COMPARISON OF STATOR CONFIGURATIONS

The relative merit of the stator configurations which were tested with respect to stiffness, net damping, and leakage characteristics is the subject of this section. The K_{ef} and C_{ef} parameters of the preceding sections are used as a measure of the direct stiffness and net damping. The leakage coefficient C_L is defined using the conventional discharge coefficient C_d definition

$$\Delta P = C_d \frac{\rho V^2}{2} \quad (9)$$

which yields

$$Q = 2\pi R \bar{C} V = \left(\frac{\bar{C}}{R}\right) C_d^{-\frac{1}{2}} \cdot 2\pi R^2 \sqrt{\frac{2\Delta P}{\rho}} = C_L \cdot 2\pi R^2 \sqrt{\frac{2\Delta P}{\rho}}$$

where \bar{C} is the average seal clearance. Hence,

$$C_L = \left(\frac{\bar{C}}{R}\right) C_d^{-\frac{1}{2}} = Q \left(2\pi R^2 \sqrt{\frac{2\Delta P}{\rho}}\right) \quad (10)$$

The coefficient C_L is a nondimensional relative measure of the leakage to be expected through seals having the same radius.

Figures 15 through 17 illustrate C_{ef} , K_{ef} , and C_L for the smooth and Rocketdyne-knurled seals at $C_r = .394$ mm. Observe that the stiffness and damping values of the two seals are comparable, but that the smooth seal leaks substantially more. Figures 18 through 20 illustrate C_{ef} , K_{ef} , and C_L for all of the seals tested with the minimum clearance $C_r = .527$ mm. In comparison to the results for $C_r = .394$ mm, leakage is increased, while K_{ef} and C_{ef} are reduced. The relative merits of the stator configurations can be evaluated from the data of table 5 below

ORIGINAL PAGE IS
OF POOR QUALITY

□ ROCKETDYNE STATOR / SMOOTH ROTOR ($C = .3937$ mm)
 ○ SMOOTH STATOR / SMOOTH ROTOR ($C = .3937$ mm)

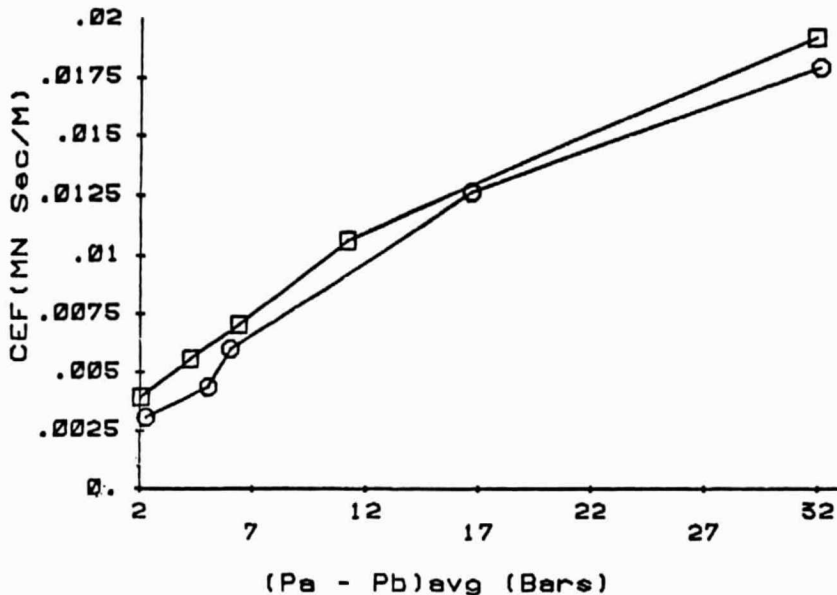


Figure 15. C_{ef} versus ΔP for the smooth and Rocketdyne-knurled inserts at $C_r = .394$ mm.

□ ROCKETDYNE STATOR / SMOOTH ROTOR ($C = .3937$ mm)
 ○ SMOOTH STATOR / SMOOTH ROTOR ($C = .3937$ mm)

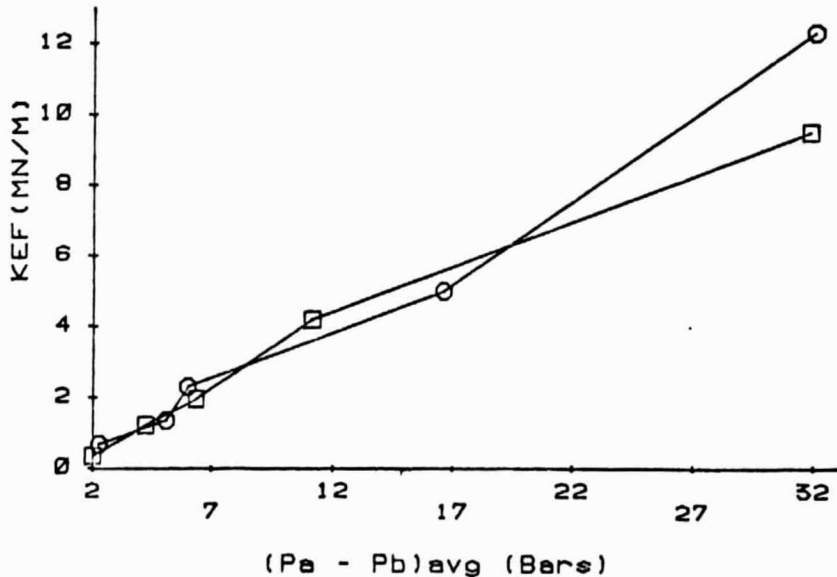


Figure 16. K_{ef} versus ΔP for the smooth and Rocketdyne-knurled inserts at $C_r = .394$ mm.

ORIGINAL PAGE IS
OF POOR QUALITY

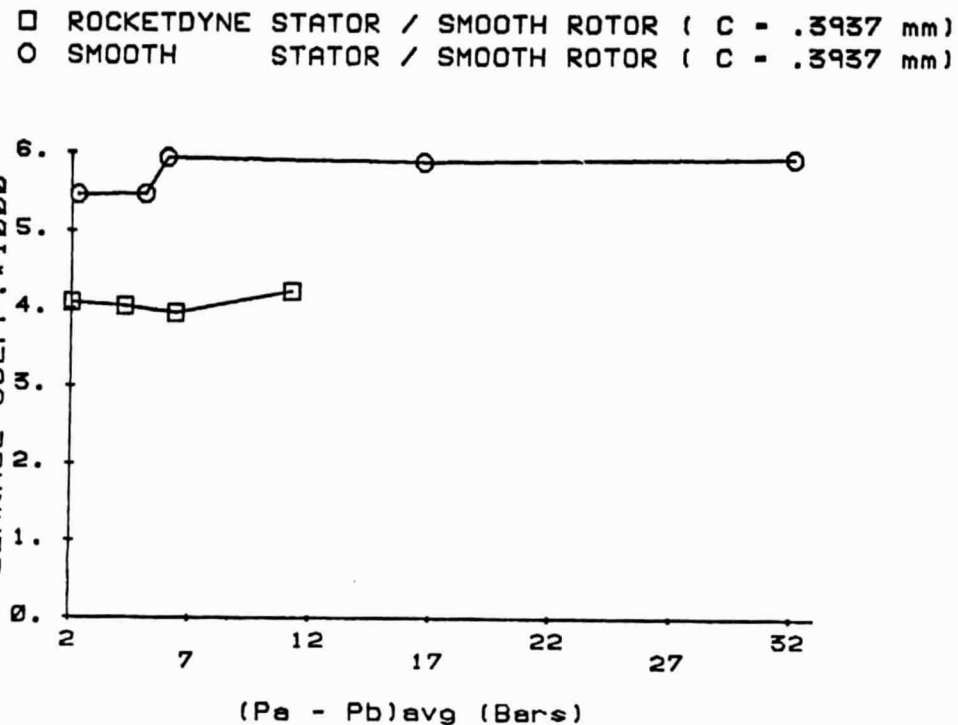


Figure 17. $C_L \times 1,000$ versus ΔP for the smooth and Rocketdyne-knurled inserts at $C_r = .394$ mm.

- \square ROCKETDYNE STATOR ($C = .5271$ mm)
- \circ SMOOTH STATOR ($C = .5271$ mm)
- Δ AXIALLY GROOVED STATOR WITH END SEALS($C_m = .8511$ mm)
- $+$ DIAMOND GRID STATOR ($C_m = .889$ mm)
- \diamond DIAMOND GRID STATOR WITH END SEALS ($C_m = .8164$ mm)
- \blacksquare ROUGH STATOR : HOLE PATTERN 1

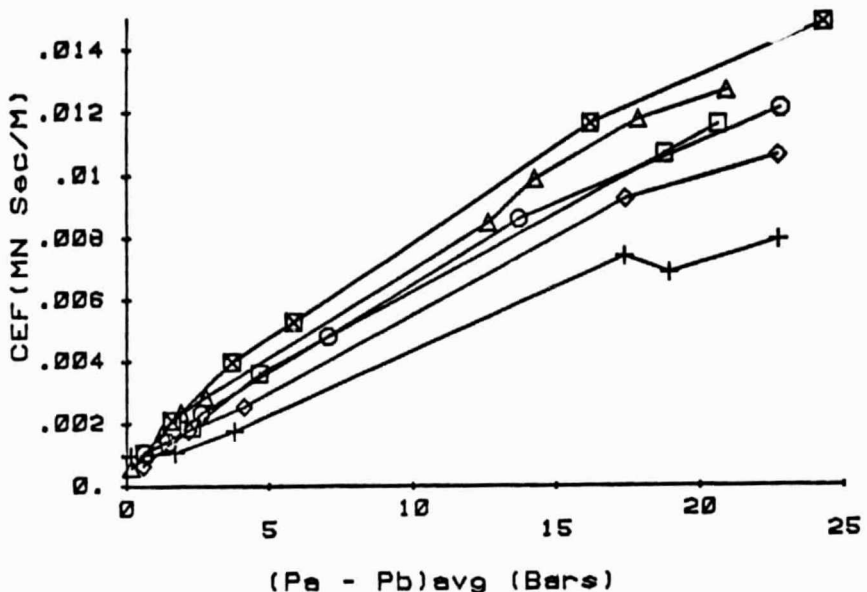


Figure 18. C_{ef} versus ΔP for all stator inserts tested with the minimum radial clearance, $C_r = .527$ mm.

- \square ROCKETDYNE STATOR ($C = .5271$ mm)
- \circ SMOOTH STATOR ($C = .5271$ mm)
- Δ AXIALLY GROOVED STATOR WITH END SEALS($C_m = .8511$ mm)
- $+$ DIAMOND GRID STATOR ($C_m = .889$ mm)
- \diamond DIAMOND GRID STATOR WITH END SEALS ($C_m = .8164$ mm)
- \blacksquare ROUGH STATOR : HOLE PATTERN 1

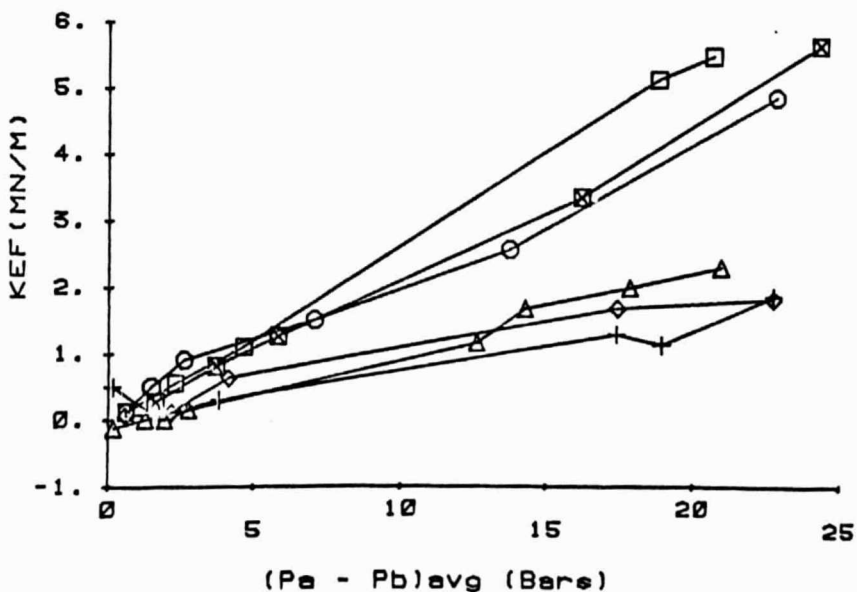


Figure 19. K_{ef} versus ΔP for all stator inserts tested with the minimum radial clearance, $C_r = .527$ mm.

- ROCKETDYNE STATOR ($C = .5271 \text{ mm}$)
- SMOOTH STATOR ($C = .5271 \text{ mm}$)
- △ AXIALLY GROOVED STATOR WITH END SEALS ($C_m = .8511 \text{ mm}$)
- + DIAMOND GRID STATOR ($C_m = .889 \text{ mm}$)
- ◊ DIAMOND GRID STATOR WITH END SEALS ($C_m = .8164 \text{ mm}$)
- ☒ ROUGH STATOR : HOLE PATTERN 1

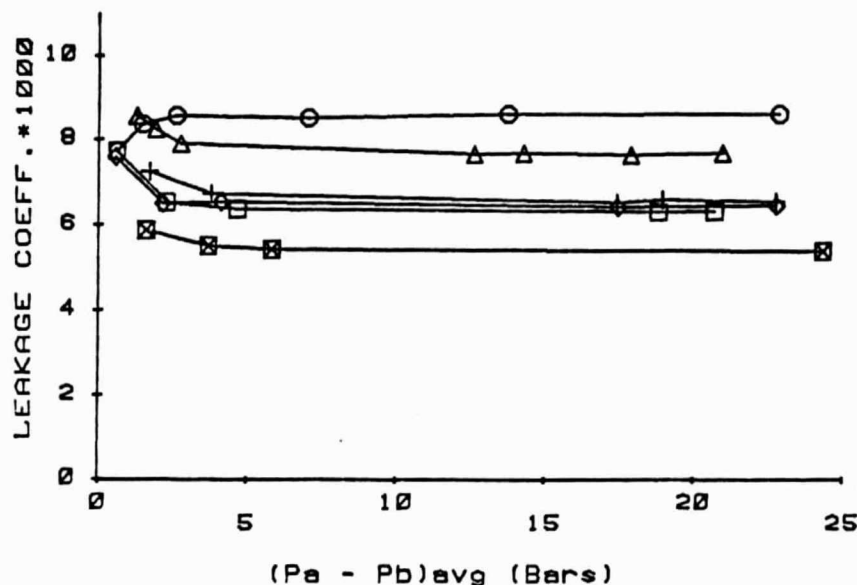


Figure 20. $C_L \times 1000$ versus ΔP for the stator inserts tested with the minimum radial clearance, $C_r = .527 \text{ mm}$.

	K_{ef} $\overline{K_{ef}}$ (max)	C_{ef} $\overline{C_{ef}}$ (max)	C_L $\overline{C_L}$ (max)
Smooth	.82	.86	1.
Rocketdyne	1.0	.86	.73
Axially grooved with end seals	.51	.94	.89
Diamond grid	.40	.58	.76
Diamond grid with end seals	.43	.74	.74
Round-hole pattern	.86	1.0	.63

Table 5. Comparison of stiffness, damping, and leakage for six stators for $C_r = .527$ mm.

Note that leakage is directly proportional to C_L ; hence, a minimum C_L is generally to be desired, and the round-hole-pattern seal is the best and the smooth seal stator the worst of those tested. From a rotordynamics viewpoint, C_{ef} should be maximized and the round-hole pattern is again superior. The question of optimum stiffness values is not so straightforward. In some rotodynamic applications, high stiffness is desirable, while for others lower stiffness values are better; e.g., in linear analysis of the HPOTP, comparison of an axially-grooved stator with the Rocketdyne stator in the rear-wear-ring seal of the boost-impeller showed both a substantial reduction in FPL bearing loads and an increase in the predicted linear OSI (Onset Speed of Instability). Observe from table 5 that the axially-grooved seal has one half the direct stiffness of the Rocketdyne stator but approximately 10% more damping. In other applications, a maximum stiffness seal might be preferable.

The results of table 5 show a generally inferior performance for the diamond-grid pattern. Tests show that the grid pattern is very effective in increasing the relative roughness of the stator. However, in creating the

"posts" the net flow area is increased, which also increases the average clearance. Hence, despite the increased roughness, the leakage performance is on a par with the Rocketdyne stator and both the stiffness and damping are reduced. Clearly, holes into the stator are more desireable for developing stator roughness than a relieving operation which yields "posts" or "prisms."

A systematic variation of stator roughness with an analytic model, holding the clearance constant, shows that damping increases and leakage decreases as roughness is increased. However, stiffness first increases and then decreases, eventually becoming negative. The results of table 5 show this type of trend with the stiffness increasing from the smooth stator to the Rocketdyne stator and then decreasing with the additional roughness of the round-hold-pattern stator. Hence, one would anticipate that increasing the round-hold-pattern roughness, e.g., by increasing the number of holes, would further reduce both leakage and the direct stiffness values but increase the effective damping values. A thorough understanding of the variation of surface roughness with hole-area density and hole geometry should permit the selection of a seal which has specified (within limits) ratios of C_{ef}/K_{ef} .

CONCLUSIONS AND RECOMMENDATION

The combined computational-analytical program carried out in this study support the following conclusions:

Experiment Versus Theory

- (a) Seals tested show substantially higher stiffness than predicted.
- (b) The theory does a generally adequate job of predicting the effective damping of a seal.
- (c) Effective added-mass coefficients from measurements are much larger than predicted.

Relative Merits of Seal Configurations

- (a) The round-hole-pattern stator yields the least leakage and highest effective damping of all the configurations tested.
- (b) The Rocketdyne-knurled stator yields the highest direct stiffness of all the configurations tested.

Continued testing of the round-hole-pattern stator configuration to systematically examine the influence of parametric variation is recommended.

REFERENCES

1. D. W. Childs, "SSME HPFTP Interstage Seals: Analysis and Experiments for Leakage and Reaction-Force Coefficients," Progress Report, NAS8-33716, Texas A&M University-Turbomachinery Laboratories Report, Seal-1-83, 15 February 1983.
2. D. W. Childs, "SSME HPFTP Interstage Seals: Analysis and Experiments for Leakage and Reaction-Force Coefficients," Supplementary Progress Report, NASA Contract NAS8-33716, Texas A&M University-Turbomachinery Laboratories Report Seal-2-83, 15 July 1983.
3. D. W. Childs, "SSME Seal Program: Leakage Tests for Helically-Grooved Seals," Progress Report NASA Contract NAS8-33716, Texas A&M University-Turbomachinery Laboratories Report, Seal-3-83, 1 November 1983.
4. G. L. von Pragenu, "Damping Seals for Turbomachinery," NASA Technical Paper 1987, 1982.
5. D. W. Childs and C-H Kim, "Analysis and Testing of Turbulent Annular Seals with Different, Directionally Homogeneous Surface Roughness Treatments for Rotor and Stator Elements," in preparation for submittal to ASME-ASLE Joint Lubrication Conference.
6. H. Stephen and K. Lucas, Viscosity of Dense Fluids, p. 59, Plenum Press, New York-London.
7. Y. Yamada, "Resistance of Flow through Annulus with an Inner Rotating Cylinder," Bul. J. S. M. E., Vol. 5, no. 18, pp. 302-310, 1962.
8. G. G. Hirs, "A Bulk-Flow Theory for Turbulence in Lubricant Films," ASME J. Lubrication Technology, pp. 137-146, April 1973.
9. C. F. Colebrook, "Turbulent Flow in Pipes with Particular Reference to the Transition Region Between the Smooth and Rough Pipe Laws," J. of the Institute of Civil Engineering (London), Vol. 11, pp. 133-156, 1938-1939.
10. D. W. Childs, "Finite-Length Solutions for the Rotordynamic Coefficients of Constant-Clearance and Convergent-Tapered Annular Seals," submitted to Int. Conference of Vibrations in Rotating Machinery, 1984.

APPENDIX A

ANALYSIS AND TESTING FOR ROTORDYNAMIC COEFFICIENTS
OF TURBULENT ANNULAR SEALS WITH DIFFERENT,
DIRECTIONALLY-HOMOGENEOUS SURFACE ROUGHNESS TREATMENTS
FOR ROTOR AND STATOR ELEMENTS.

D. W. Childs

and

Chang-Ho Kim

Department of Mechanical Engineering
Texas A&M University
College Station, Texas 77843

ABSTRACT

A combined analytical-computational method is developed to calculate the transient pressure field and dynamic coefficients for high-pressure annular seal configurations which may be used in interstage and neck-ring seals of multistage centrifugal pumps. The solution procedure applies to constant-clearance or convergent-tapered geometries which may have different (but directionally-homogeneous) surface-roughness treatments on the stator or rotor seal elements. It applies in particular to so-called "damper-seals" which employ smooth rotors and deliberately-roughened stator elements to enhance rotor stability.

Hirs' turbulent lubrication equations are modified slightly to account for different surface-roughness conditions on the rotor and stator. A perturbation analysis is employed in the eccentricity ratio to develop zeroth and first order perturbation

equations. The zeroth-order equations define both the leakage and the development of circumferential flow due to shear forces at the rotor and stator surfaces. The first-order equations define perturbations in the pressure and axial and circumferential velocity fields due to small relative motion between the seal rotor and stator. The solution applies for small motion about a centered position and does not employ linearization with respect to either the taper angle or the degree of swirl, i.e., the difference between the circumferential velocity at a given axial position and the asymptotic circumferential-velocity solution corresponding to fully developed flow.

INTRODUCTION

Figure 1 illustrates the two seal types which have the potential for developing significant rotor forces. The neck- or wear-ring seals are provided to reduce the leakage flow back along the front surface of the impeller face, while the interstage seal reduces the leakage from an impeller inlet back along the shaft to the backside of the preceding impeller. Pump seals may be geometrically similar to plain journal bearings, but typically have clearance to radius ratios on the order of 0.005 as compared to 0.001 for bearings. Because of the clearances, and normally-experienced pressure differentials, fully-developed turbulent flow normally exists in pump seals.

As related to rotordynamics, analysis of seals has the objective of defining the reaction force acting on a rotor as a consequence of shaft motion. For small motions about a centered position, the relation between the reaction-force components and shaft motion may be expressed by

$$-\begin{Bmatrix} F_x \\ F_y \end{Bmatrix} = \begin{bmatrix} K & k \\ -k & K \end{bmatrix} \begin{Bmatrix} x \\ y \end{Bmatrix} + \begin{bmatrix} c & c \\ -c & C \end{bmatrix} \begin{Bmatrix} \dot{x} \\ \dot{y} \end{Bmatrix} + \begin{bmatrix} M & m \\ -m & M \end{bmatrix} \begin{Bmatrix} \ddot{x} \\ \ddot{y} \end{Bmatrix} \quad (1)$$

The off-diagonal coefficients in Eq. (1) are referred to as "cross-coupled" and arise due to fluid rotation within the seal. Seals, unlike plain journal bearings, develop significant direct stiffness values K in the centered, zero-eccentricity position due to the distribution between (a) inlet losses, and

(b) the axial pressure gradient due to wall-friction losses.

Lomakin [1] initially pointed out the phenomenon. Both analysis [2] and experiments [3] have shown that Eq. (1) holds for fairly large eccentricities on the order of 0.5; i.e., the dynamic coefficients tend to be relatively insensitive to changes in the static-eccentricity ratio.

Prior analytical and experimental developments have generally examined "smooth" seals where both stator and rotor elements of the seal are assumed to have the same nominally smooth surfaces. A review of the analytical and experimental developments for this type of seal is provided in references [4] and [5] and will not be repeated here. The subject of this investigation is the so-called "damper-seal" configuration recently proposed by von Pragenau [6], which employs a smooth rotor and a deliberately surface-roughened stator element. For the same surface roughness on the rotor and stator, the asymptotic, circumferential, bulk-flow velocity is assumed to be $Rw/2$ in the centered position because (a) the radial velocity distribution is assumed to be symmetrical about the midplane, and (b) the circumferential velocity is zero at the stator wall and Rw at the rotor wall. Von Pragenau's analysis demonstrates that the damper seal yields a lower asymptotic circumferential velocity which implies a reduction in the destabilizing cross-coupled stiffness coefficient k and a consequential improvement in rotordynamic stability.

Von Pragenau employs an approximate "short-seal" analysis

to develop analytical expressions for the rotordynamic coefficients of constant clearance seals. The development of these analytical expressions is lengthy and difficult. The combined analytical-computational approach used in this development yields an exact solution to the governing equations for both constant-clearance and convergent-tapered seals with significantly less labor. Following a slight modification to Hirs' governing equation to account for different surface-roughness conditions on the rotor and stator, the analysis procedure is basically that of references [4] and [5].

GOVERNING EQUATIONS

Figure 2 illustrates a differential element of fluid having dimensions $Rd\theta$, dz , and $H(z, \theta, t)$. The upper and lower surfaces of the element correspond to the rotor and stator seal elements and have velocities of $R\omega$ and zero, respectively. The bulk velocity components of the fluid are U_θ and U_z ; i.e., these are the averages across the fluid film height H of the circumferential and axial fluid velocities. The essence of Hirs' formulation is the definition of the wall shear stress τ_w as the following empirical function of the bulk flow velocity V_w relative to the wall

$$\tau_w = \rho \frac{V_w^2}{2} no \left(\frac{2\rho V_w H}{\mu} \right)^{mo} = \rho \frac{V_w^2}{2} no R_{ao}^{mo} \quad (2)$$

The bulk flow velocities relative to the rotor and stator are, respectively

$$\begin{aligned} V_r &= (U_\theta - R\omega) \underline{\varepsilon}_\theta + U_z \underline{\varepsilon}_z \\ V_s &= U_\theta \underline{\varepsilon}_\theta + U_z \underline{\varepsilon}_z \end{aligned} \quad (3)$$

Hence, the shear stress at the rotor and stator are

$$\begin{aligned} \tau_r &= \rho \frac{V_r^2}{2} nr \left(\frac{2\rho V_r H}{\mu} \right)^{mr} \\ \tau_s &= \rho \frac{V_s^2}{2} ns \left(\frac{2\rho V_s H}{\mu} \right)^{ms} \end{aligned} \quad (4)$$

Hirs' formulation assumes that the surface roughness is the same on the stator and rotor; hence, the same empirical

constants m_o, n_o apply to both surfaces. The formulation of Eq. (4) accounts for different surface roughnesses in the stator elements via the empirical constants $(m_r, n_r), (m_s, n_s)$ for the rotor and stator surfaces.

The components of wall shear surface stress in the Z and $R\theta$ directions are

$$\tau_{r\theta} = \tau_r (U_\theta - R\omega) / V_r; \quad \tau_{rz} = \tau_r U_z / V_r$$

$$V_r = [(U_\theta - R\omega)^2 + U_z^2]^{1/2}$$

(5)

$$\tau_{s\theta} = \tau_s U_\theta / V_s; \quad \tau_{sz} = \tau_s U_z / V_s$$

$$V_s = (U_\theta^2 + U_z^2)^{1/2}$$

Summing forces in the Z and $R\theta$ directions for the free-body diagram of Figure 2(b) yields the following momentum equations:

$$\begin{aligned} -H \frac{\partial p}{\partial Z} &= \frac{n_s}{2} \rho U_z^2 R_a^{m_s} \left[1 + (U_\theta / U_z)^2 \right]^{\frac{m_s+1}{2}} \\ &+ \frac{n_r}{2} \rho U_z^2 R_a^{m_r} \left\{ 1 + [(U_\theta - R\omega) / U_z]^2 \right\}^{\frac{m_r+1}{2}} \\ &+ \rho H \left[\frac{\partial U_z}{\partial t} + \frac{U_\theta}{R} \frac{\partial U_z}{\partial \theta} + U_z \frac{\partial U_z}{\partial Z} \right] \end{aligned} \quad (6a)$$

$$- \frac{H}{R} \frac{\partial p}{\partial \theta} = \frac{n_s}{2} \rho U_z U_\theta R_a^{m_s} \left[1 + (U_\theta / U_z)^2 \right]^{\frac{m_s+1}{2}}$$

ORIGINAL PAGE IS
OF POOR QUALITY

$$\begin{aligned} &+ \frac{n_r}{2} \rho U_z (U_\theta - R\omega) R_a^{m_r} \left\{ 1 + [(U_\theta - R\omega) / U_z]^2 \right\}^{\frac{m_r+1}{2}} \\ &+ \rho H \left[\frac{\partial U_\theta}{\partial t} + \frac{U_\theta}{R} \frac{\partial U_\theta}{\partial \theta} + U_z \frac{\partial U_\theta}{\partial Z} \right] \end{aligned} \quad (6b)$$

The bulk-flow continuity equation is

ORIGINAL PAGE IS
OF POOR QUALITY

$$\frac{\partial H}{\partial t} + \frac{1}{R} \frac{\partial (HU_\theta)}{\partial \theta} + \frac{\partial (HU_z)}{\partial z} = 0 \quad (6c)$$

These equations may be nondimensionalized by introducing the following variables:

$$u_z = U_z / \bar{V}, \quad u_\theta = U_\theta / R\omega, \quad \tilde{p} = p / \rho \bar{V}^2$$

$$h = H / \bar{C}, \quad \tau = t / T, \quad z = Z / L \quad (7)$$

$$T = L / \bar{V}, \quad b = \bar{V} / R\omega$$

where \bar{C} and \bar{V} are the average clearance and axial velocity, respectively. The resultant equations are

$$\begin{aligned} -h \frac{\partial \tilde{p}}{\partial z} &= \frac{ns}{2} \left(\frac{L}{\bar{C}} \right) R_a^{ms} \left[1 + \left(\frac{u_\theta}{bu_z} \right)^2 \right]^{\frac{ms+1}{2}} u_z^2 \\ &\quad + \frac{nr}{2} \left(\frac{L}{\bar{C}} \right) R_a^{mr} \left[1 + \left(\frac{u_\theta - 1}{bu_z} \right)^2 \right]^{\frac{mr+1}{2}} u_z^2 \\ &\quad + h \left[\frac{\partial u_z}{\partial \tau} + u_\theta (\omega T) \frac{\partial u_z}{\partial \theta} + u_z \frac{\partial u_z}{\partial z} \right] \quad (8) \\ -b \left(\frac{L}{\bar{R}} \right) h \frac{\partial \tilde{p}}{\partial \theta} &= \frac{ns}{2} \left(\frac{L}{\bar{C}} \right) R_a^{ms} \left[1 + \left(\frac{u_\theta}{bu_z} \right)^2 \right]^{\frac{ms+1}{2}} u_z u_\theta \\ &\quad + \frac{nr}{2} \left(\frac{L}{\bar{C}} \right) R_a^{mr} \left[1 + \left(\frac{u_\theta - 1}{bu_z} \right)^2 \right]^{\frac{mr+1}{2}} u_z (u_\theta - 1) \\ &\quad + h \left[\frac{\partial u_\theta}{\partial \tau} + u_\theta (\omega T) \frac{\partial u_\theta}{\partial \theta} + u_z \frac{\partial u_\theta}{\partial z} \right] \\ \frac{\partial h}{\partial \tau} + (\omega T) \frac{\partial (hu_\theta)}{\partial \theta} + \frac{\partial (hu_z)}{\partial z} &= 0 \end{aligned}$$

PERTURBATION EQUATIONS

Seal Geometry

Figure 3 illustrates the geometry for a tapered seal.

At the centered position, the clearance function is defined by

$$H_0(z) = (\bar{C} + \frac{\alpha L}{2}) - \alpha z = [1 + q(1 - 2z)] \bar{C} = f \bar{C} \quad (9)$$

where α is the taper angle, and

$$\bar{C} = (C_0 + C_1)/2, \quad q = \frac{\alpha L}{2\bar{C}} = \frac{C_0 - C_1}{C_0 + C_1} \quad (10)$$

The parameter q is a measure of the degree of taper in a seal and varies from zero, for a constant-clearance configuration, to approximately 0.4 for a maximum-stiffness seal design [7].

Perturbation Analysis

The governing equations (Eq. (6)) define the bulk-flow velocity components (u_θ, u_z) and the pressure, p , as a function of the spatial variables ($R\theta, z$) and time, t . An expansion of these equations in the perturbation variables

$$\begin{aligned} u_z &= u_{z0} + \epsilon u_{z1}, \quad h = h_0 + \epsilon h_1 \\ u_\theta &= u_{\theta0} + \epsilon u_{\theta1}, \quad \tilde{p} = \tilde{p}_0 + \epsilon \tilde{p}_1 \end{aligned} \quad (11)$$

where $\epsilon = e/\bar{C}$ is the eccentricity ratio yields the following equations.

Zeroth-Order Equations:

(a) Axial-Momentum Equation

$$\frac{d\tilde{p}_0}{dz} = - \left[(a_{0s} \sigma_s + a_{0r} \sigma_r) + 4q \right] / 2f^3 \quad (12a)$$

(b) Circumferential-Momentum Equation

$$\frac{du_{\theta 0}}{dz} = - \left[a_{0r} \sigma_r (u_{\theta 0} - 1) + a_{0s} \sigma_s u_{\theta 0} \right] / 2f \quad (12b)$$

(c) Continuity Equation

$$u_{z0} = 1/f \quad (12c)$$

First-Order Equations

(a) Axial-Momentum Equation

$$\begin{aligned} \frac{\partial \tilde{p}_1}{\partial z} &= h_1 A_{1z} - u_{\theta 1} A_{2z} - \bar{u}_{z1} A_{3z} \\ &- \left\{ \frac{\partial u_{z1}}{\partial \tau} + (\omega T) u_{\theta 0} \frac{\partial u_{z1}}{\partial \theta} + \frac{1}{f} \frac{\partial \bar{u}_{z1}}{\partial z} \right\} \end{aligned} \quad (13a)$$

(b) Circumferential-Momentum Equation

$$\begin{aligned} b(\frac{L}{R}) \frac{\partial \tilde{p}_1}{\partial \theta} &= h_1 A_{1\theta} - u_{\theta 1} A_{2\theta} - u_{z1} A_{3\theta} \\ &- \left\{ \frac{\partial u_{\theta 1}}{\partial \tau} + (\omega T) u_{\theta 0} \frac{\partial u_{\theta 1}}{\partial \theta} + \frac{1}{f} \frac{\partial u_{\theta 1}}{\partial z} \right\} \end{aligned} \quad (13b)$$

ORIGINAL PAGE IS
OF POOR QUALITY

(c) Continuity Equation

$$\frac{\partial u_{z1}}{\partial z} + (\omega T) \frac{\partial u_{\theta 1}}{\partial \theta} - \frac{2q}{f} u_{z1} = -\frac{1}{f} \left[\frac{2qh_1}{f^2} + (\omega T) u_{\theta 0} \frac{\partial h_1}{\partial \theta} + \frac{\partial h_1}{\partial \tau} \right] \quad (13c)$$

Most of the parameters of these equations are defined in Appendix A. The quantities σ_s, σ_r are defined by

$$\sigma_s = \left(\frac{L}{C}\right) \lambda_s, \quad \sigma_r = \left(\frac{L}{C}\right) \lambda_r \quad (14)$$

where the wall friction factors are defined by

$$\lambda_s = nsR_{a0}^{ms} \left(1 + \frac{1}{4b^2}\right)^{\frac{1+ms}{2}}, \quad \lambda_r = nrR_{a0}^{mr} \left(1 + \frac{1}{4b^2}\right)^{\frac{1+mr}{2}} \quad (15)$$

These expressions correspond to Yamada's [8] test correlation for flow between rotating annuli.

SOLUTION PROCEDURES

Zeroth-Order Equations

The zeroth-order equations define the steady-state leakage and the circumferential velocity development $u_{\theta 0}(z)$ due to wall shear. The governing equations, Eqs. (12), are coupled and nonlinear through the dependency of the coefficients a_{0r} , a_{0s} , $u_{\theta 0}$ and \bar{V} . The equations must be solved iteratively to determine the average leakage velocity \bar{V} corresponding to a specified pressure drop ΔP and the circumferential velocity distribution $U_{\theta 0}(z)$. The resultant solution defines the leakage coefficient C_d of the leakage- ΔP relationship

$$\Delta P = C_d \frac{\rho \bar{V}^2}{2} \quad (16)$$

The pressure drop at the entrance is defined by

$$\Delta P_0 = \frac{\rho \bar{V}^2}{2} \frac{(1+\xi)}{(1+q)^2} \quad (17)$$

where ξ is an entrance-loss coefficient which is generally on the order of 0.1 to 0.5.

First-Order Equations

The governing first-order equations define $p_1(z, \theta, \tau)$

$u_{z1}(z, \theta, \tau)$ and $u_{\theta 1}(z, \theta, \tau)$ resulting from the seal clearance functions $h_1(\theta, \tau)$. The clearance H is defined in terms of the components of the seal-journal displacement vector (X, Y) by

$$H = H_0 - X \cos\theta - Y \sin\theta$$

Hence, by comparison to Eq. (11),

$$\epsilon h_1 = -x \cos\theta - y \sin\theta \quad (18)$$

where

$$x = X/\bar{C}, \quad y = Y/\bar{C}$$

Note that h_1 is not a function of z , and its time dependency arises from the displacement variables $x(t)$, $y(t)$.

To satisfy circumferential continuity conditions, the following solution format is assumed:

$$u_{z1}(z, \theta, \tau) = u_{z1C}(z, \tau) \cos\theta + u_{z1S}(z, \tau) \sin\theta$$

$$u_{\theta 1}(z, \tau, \theta) = u_{\theta 1C}(z, \tau) \cos\theta + u_{\theta 1S}(z, \tau) \sin\theta \quad (19)$$

$$\tilde{p}_1(z, \theta, \tau) = \tilde{p}_{1C}(z, \tau) \cos\theta + \tilde{p}_{1S}(z, \tau) \sin\theta$$

Substituting from Eq. (19) into Eq. (13) eliminates θ as an independent variable, and yields six real equations. By introducing the complex variables

$$\hat{u}_{z1} = \bar{u}_{z1c} + ju_{z1s}$$

$$\hat{u}_{\theta 1} = \bar{u}_{\theta 1c} + ju_{\theta 1s}$$

(20)

$$\hat{p}_1 = \bar{p}_{1c} + j\bar{p}_{1s}$$

$$\frac{\hat{h}_1}{\epsilon} = \frac{x}{\epsilon} + j \frac{y}{\epsilon}$$

into these equations, the following complex equations are obtained:

$$\begin{aligned}
 -\frac{\partial \hat{p}_1}{\partial z} &= A_{1z} \left(\frac{\hat{h}_1}{\epsilon} \right) + A_{2z} \hat{u}_{\theta 1} + A_{3z} \hat{u}_{z1} \\
 &+ \frac{\partial \hat{u}_{z1}}{\partial \tau} - j(\omega T) u_{\theta 0} \hat{u}_{z1} + \frac{1}{f} \frac{\partial \hat{u}_{z1}}{\partial z} \\
 j b \left(\frac{L}{R} \right) \hat{p}_1 &= A_{1\theta} \left(\frac{\hat{h}_1}{\epsilon} \right) + A_{2\theta} \hat{u}_{\theta 1} + A_{3\theta} \hat{u}_{z1} \quad (21) \\
 &+ \frac{\partial \hat{u}_{\theta 1}}{\partial \tau} - j(\omega T) u_{\theta 0} \hat{u}_{\theta 1} + \frac{1}{f} \frac{\partial \hat{u}_{\theta 1}}{\partial z}
 \end{aligned}$$

$$\begin{aligned}
 \frac{\partial \hat{u}_{z1}}{\partial z} - j(\omega T) \hat{u}_{\theta 1} - \frac{2q}{f} \hat{u}_{z1} &= \frac{2q}{f^3} \left(\frac{\hat{h}_1}{\epsilon} \right) - j \frac{(\omega T)}{f} u_{\theta 0} \left(\frac{\hat{h}_1}{\epsilon} \right) \\
 &+ \frac{1}{f} \frac{\partial}{\partial \tau} \left(\frac{\hat{h}_1}{\epsilon} \right)
 \end{aligned}$$

The time dependency in these equations is eliminated by assuming a harmonic seal motion of the form

$$\hat{h}_1 = \frac{R_0}{C} e^{j\Omega t} = r_0 e^{j\Omega T\tau} \quad (22)$$

where r_0 is a real constant. The associated harmonic solution can then be stated

$$\hat{u}_{z1}(z, \tau) = \bar{u}_{z1}(z) e^{j\Omega T\tau}$$

$$\hat{u}_{\theta 1}(z, \tau) = \bar{u}_{\theta 1}(z) e^{j\Omega T\tau} \quad (23)$$

$$\hat{p}_1(z, \tau) = \bar{p}_1(z) e^{j\Omega T\tau}$$

Substitution from Eqs. (22) and (23) into Eq. (21) yields

$$\frac{d}{dz} \begin{Bmatrix} \bar{u}_{z1} \\ \bar{u}_{\theta 1} \\ \bar{p}_1 \end{Bmatrix} + [A] \begin{Bmatrix} \bar{u}_{z1} \\ \bar{u}_{\theta 1} \\ \bar{p}_1 \end{Bmatrix} = \left(\frac{r_0}{\epsilon} \right) \begin{Bmatrix} g_1 \\ g_2 \\ g_3 \end{Bmatrix} \quad (24)$$

where

$$[A] = \begin{bmatrix} -2q/f & -j(\omega T) & 0 \\ fA_{30} & f(A_{23} + j\Gamma T) & -jfb(L/R) \\ (A_{3z} + 2q/f^2 + j\Gamma T) & A_{2z} + j(\omega T)/f & 0 \end{bmatrix} \quad (25)$$

$$\begin{Bmatrix} g_1 \\ g_2 \\ g_3 \end{Bmatrix} = \begin{Bmatrix} (2q/f^3 + j\Gamma T/f) \\ -fA_{10} \\ -(A_{1z} + 2q/f^4 + j\Gamma T/f^2) \end{Bmatrix}$$

and

$$\Gamma = \Omega - \omega u_{\theta 0} \quad (26)$$

The following three boundary conditions are specified for the solution of Eq. (25) :

(a) The exit pressure perturbation is zero; i.e.,

$$\bar{p}_1(L) = 0 \quad (27)$$

(b) The entrance circumferential velocity perturbation is zero; i.e.,

$$\bar{u}_{\theta 1}(0) = 0 \quad (28)$$

(c) The pressure loss at the seal entrance is defined by

$$P_s - p(0, \theta, \tau) = \frac{\rho}{2} u_z^2(0, \theta, \tau) (1+\xi),$$

which yields the following boundary condition:

$$\bar{p}_1(0) = -(1+\xi) \bar{u}_{z1}(0) / b(1+q) \quad (29)$$

Solution of the differential Eqs. (24) in terms of the boundary conditions is relatively straightforward, yielding a solution for the velocity and pressure fields of the form

$$\begin{Bmatrix} \bar{u}_{z1} \\ \bar{u}_{\theta 1} \\ \bar{p}_1 \end{Bmatrix} = \left(\frac{r_0}{\epsilon} \right) \begin{Bmatrix} f_{1C} + j f_{1S} \\ f_{2C} + j f_{2S} \\ f_{3C} + j f_{3S} \end{Bmatrix} \quad (30)$$

ORIGINAL PAGE IS
OF POOR QUALITY

APPENDIX A: PERTURBATION COEFFICIENTS

$$B_s a_{0s} = \left[1 + \left(u_{\theta 0} / bu_{z0} \right)^2 \right]^{\frac{ms+1}{2}}, \quad B_s = \left(1 + \frac{1}{4b^2} \right)^{\frac{ms+1}{2}}$$

$$B_r a_{0r} = \left\{ 1 + \left[\left(u_{\theta 0}^{-1} \right) / bu_{z0} \right]^2 \right\}^{\frac{mr+1}{2}}, \quad B_r = \left(1 + \frac{1}{4b^2} \right)^{\frac{mr+1}{2}}$$

$$B_s a_{1s} = \left[1 + \left(u_{\theta 0} / bu_{z0} \right)^2 \right]^{\frac{ms-1}{2}}$$

$$B_r a_{1r} = \left\{ 1 + \left[\left(u_{\theta 0}^{-1} \right) / bu_{z0} \right]^2 \right\}^{\frac{mr-1}{2}}$$

$$A_{1z} = \left[a_{0s} \sigma_s (1-ms) + a_{0r} \sigma_r (1-mr) \right] / 2f^4$$

$$A_{2z} = \left[(ms+1) \sigma_s a_{1s} u_{\theta 0} + (mr+1) \sigma_r a_{1r} (u_{\theta 0}^{-1}) \right] / 2b^2 f$$

$$A_{3z} = \left[a_{0s} \sigma_s (2+ms) + a_{0r} \sigma_r (2+mr) \right] / 2f^2 + 2q/f^2 - \left[a_{1s} \sigma_s (1+ms) u_{\theta 0}^2 + a_{1r} \sigma_r (1+mr) (u_{\theta 0}^{-1})^2 \right] / 2b^2$$

$$A_{1\theta} = \left[\sigma_s a_{0s} u_{\theta 0} (1-ms) + \sigma_r a_{0r} (u_{\theta 0}^{-1}) (1-mr) \right] / 2f^3$$

$$A_{2\theta} = (\sigma_s a_{0s} + \sigma_r a_{0r}) / 2f^2 + \left[\sigma_s (1+ms) a_{1s} u_{\theta 0}^2 + \sigma_r (1+mr) a_{1r} (u_{\theta 0}^{-1})^2 \right] / 2b^2$$

$$A_{3\theta} = \left[\sigma_s^{ms} a_{0s} u_{\theta 0} + \sigma_r^{mr} a_{0r} (u_{\theta 0}^{-1}) \right] / 2f - f \left[\sigma_s a_{1s} (1+ms) u_{\theta 0}^3 + \sigma_r a_{1r} (1+mr) (u_{\theta 0}^{-1})^3 \right] / 2b^2$$

ORIGINAL PAGE IS
OF POOR QUALITY

SMOOTH STATOR / SMOOTH ROTOR C(RADIAL) = 0.3937 mm
SEAL TEST HEADER DATA
DR. D. CHILDS TEXAS A&M SEP. 83

Case	Pa-Pb (Bars)	RHO (Kg/M ³)	MU (N sec/M ²)	MDOT (Kg/sec)	CPM (Cyc/min)
1.	0. 913	1557. 183	0. 148E-03	2. 337	1376.
2.	0. 989	1557. 515	0. 148E-03	2. 368	2299.
3.	1. 051	1554. 419	0. 147E-03	2. 357	3109.
4.	1. 251	1568. 484	0. 151E-03	2. 405	3797.
5.	1. 326	1567. 872	0. 151E-03	2. 412	5333.
6.	1. 356	1543. 109	0. 144E-03	2. 322	7186.
7.	2. 488	1560. 981	0. 149E-03	3. 616	3797.
8.	2. 600	1557. 983	0. 148E-03	3. 501	5310.
9.	2. 790	1558. 904	0. 148E-03	4. 125	1357.
10.	2. 939	1551. 447	0. 146E-03	4. 144	2281.
11.	3. 066	1557. 831	0. 148E-03	4. 280	3117.
12.	3. 236	1541. 985	0. 143E-03	4. 172	7186.
13.	7. 812	1543. 198	0. 143E-03	6. 771	1351.
14.	7. 951	1543. 522	0. 143E-03	6. 760	2230.
15.	8. 625	1571. 804	0. 151E-03	7. 160	3158.
16.	8. 587	1551. 913	0. 145E-03	6. 955	3810.
17.	8. 475	1549. 781	0. 145E-03	6. 902	5310.
18.	8. 566	1547. 524	0. 145E-03	6. 910	7186.
19.	15. 852	1559. 775	0. 147E-03	9. 773	1370.
20.	15. 974	1564. 021	0. 148E-03	9. 750	2290.
21.	15. 906	1562. 631	0. 148E-03	9. 689	3109.
22.	16. 128	1551. 623	0. 145E-03	9. 643	3797.
23.	16. 389	1556. 370	0. 146E-03	9. 697	5310.
24.	15. 922	1548. 772	0. 144E-03	9. 531	7186.

B.1. Test data: Operating conditions and parameters for the smooth stator; $C_r = .3937$ mm.

**ORIGINAL PAGE IS
OF POOR QUALITY**

ROCKETDYNE STATOR / SMOOTH ROTOR $C_{(RADIAL)} = 0.3937$ mm
 SEAL TEST HEADER DATA
 DR. D. CHILDS TEXAS A&M SEP. 83

Case	Pa-Pb (Bars)	RHO (Kg/M ³)	NU (N·sec/M ²)	MDOT (Kg/sec)	CPM (Cyc/min)
1.	0.784	1579.990	0.154E-03	1.702	1415.
2.	0.901	1577.513	0.154E-03	1.728	2353.
3.	0.961	1575.745	0.153E-03	1.700	3183.
4.	1.112	1571.267	0.152E-03	1.634	3810.
5.	1.131	1569.098	0.151E-03	1.657	5333.
6.	1.289	1543.178	0.143E-03	1.605	7186.
7.	1.901	1567.506	0.151E-03	2.404	1389.
8.	2.050	1569.114	0.151E-03	2.426	2317.
9.	2.102	1572.181	0.152E-03	2.417	3175.
10.	2.112	1567.193	0.151E-03	2.395	3810.
11.	2.219	1566.934	0.151E-03	2.397	5310.
12.	2.374	1546.525	0.144E-03	2.308	7186.
13.	3.036	1574.170	0.153E-03	2.897	1402.
14.	3.083	1575.572	0.153E-03	2.912	2344.
15.	3.119	1574.508	0.153E-03	2.904	3191.
16.	3.260	1576.188	0.153E-03	2.917	3797.
17.	3.270	1571.768	0.152E-03	2.880	5310.
18.	3.344	1541.128	0.143E-03	2.730	7186.
19.	5.549	1561.909	0.149E-03	4.049	1376.
20.	5.475	1560.841	0.149E-03	3.956	2290.
21.	5.513	1559.612	0.148E-03	4.060	3125.
22.	5.653	1560.837	0.149E-03	4.036	3810.
23.	5.574	1557.433	0.148E-03	4.064	4819.
24.	5.842	1547.488	0.144E-03	4.292	7186.

B.2. Test data: Operating conditions and parameters for the Rocketdyne-knurled stator; $C_r = .3937$ mm.

ORIGINAL PAGE IS
OF POOR QUALITY

25.	15. 542	1557. 750	0. 146E-03	10. 077	1351.
26.	15. 958	1563. 786	0. 148E-03	10. 099	2290.
27.	16. 084	1567. 314	0. 149E-03	10. 792	3125
28.	16. 134	1565. 638	0. 149E-03	9. 456	3797.
29.	16. 231	1565. 353	0. 149E-03	9. 168	5310.
30.	15. 713	1549. 240	0. 144E-03	10. 189	7186.

B.2. Test data: Operating conditions and parameters for the Rocketdyne-knurled stator; $C_r = .3937$ mm.

**ORIGINAL PAGE IS
OF POOR QUALITY**

SMOOTH STATOR / SMOOTH ROTOR $C = 0.5271$ mm
 SEAL TEST HEADER DATA
 DR. D. CHILDS TEXAS A&M SEP. 83

Case	Pa-Pb (Bars)	RHO (Kg/M ³)	MU (N sec/M ²)	MDOT (Kg/sec)	CPM (Cyc/min)
1.	0.215	1593.121	0.150E-03	1.744	1111.
2.	0.251	1591.023	0.158E-03	1.776	1852.
3.	0.294	1590.286	0.157E-03	1.752	2771.
4.	0.356	1586.153	0.156E-03	1.741	3681.
5.	0.417	1583.849	0.156E-03	1.694	5310.
6.	0.398	1563.640	0.150E-03	1.678	7186.
7.	0.664	1575.643	0.152E-03	2.928	1083.
8.	0.680	1575.408	0.152E-03	2.899	1807.
9.	0.727	1577.039	0.153E-03	2.924	2715.
10.	0.764	1574.946	0.152E-03	2.897	3625.
11.	0.797	1566.400	0.150E-03	2.898	5357.
12.	0.817	1562.824	0.148E-03	2.837	7186.
13.	1.205	1552.788	0.146E-03	3.882	1064.
14.	1.249	1550.623	0.145E-03	3.995	1744.
15.	1.236	1548.642	0.145E-03	3.824	2620.
16.	1.282	1547.620	0.144E-03	3.869	3488.
17.	1.419	1547.573	0.144E-03	3.980	5333.
18.	1.490	1560.932	0.148E-03	3.998	7186.
19.	3.401	1569.975	0.151E-03	6.426	1075.
20.	3.376	1568.374	0.150E-03	6.431	1780.
21.	3.429	1569.895	0.151E-03	6.381	2685.
22.	3.515	1569.496	0.151E-03	6.423	3593.
23.	3.552	1564.293	0.149E-03	6.427	5333.
24.	3.920	1579.396	0.154E-03	6.586	7186.

B.3. Test data: Operating conditions and parameters for the smooth stator; $C_r = .5271$ mm.

ORIGINAL PAGE IS
OF POOR QUALITY

25.	6. 537	1560. 894	0. 148E-03	8. 981	1079.
26.	6. 850	1564. 665	0. 149E-03	9. 099	1791.
27.	6. 811	1562. 618	0. 149E-03	9. 090	2679.
28.	6. 855	1562. 907	0. 149E-03	9. 072	3561.
29.	6. 921	1559. 107	0. 148E-03	9. 015	5310.
30.	7. 276	1571. 860	0. 151E-03	9. 259	7186.
31.	11. 399	1567. 775	0. 149E-03	11. 760	1056.
32.	11. 390	1565. 970	0. 148E-03	11. 776	1780.
33.	11. 393	1569. 418	0. 149E-03	11. 812	2667.
34.	11. 314	1569. 017	0. 149E-03	11. 732	3561.
35.	11. 444	1566. 916	0. 149E-03	11. 720	5310.
36.	11. 559	1586. 925	0. 154E-03	11. 786	7186.
37.	11. 176	1563. 172	0. 148E-03	11. 687	1053.
38.	11. 161	1562. 483	0. 148E-03	11. 649	1770.
39.	11. 176	1560. 918	0. 147E-03	11. 664	2643.
40.	11. 393	1567. 441	0. 149E-03	11. 734	3550.
41.	11. 442	1562. 253	0. 148E-03	11. 719	5310.
42.	11. 253	1555. 783	0. 146E-03	11. 554	7186.

B.3. Test data: Operating conditions and parameters for the smooth stator; $C_r = .5271$ mm.

**ORIGINAL PAGE IS
OF POOR QUALITY**

ROCKETDYNE STATOR / SMOOTH ROTOR C = 0.5271 mm
SEAL TEST HEADER DATA
DR. D. CHILDS TEXAS A&M SEP. 83

Case	Pa-Pb (Bars)	RHO (Kg/M ³)	MU (N·sec/M ²)	MDOT (Kg/sec)	CPM (Cyc/min)
1.	0.215	1593.121	0.158E-03	1.744	1111.
2.	0.251	1591.023	0.158E-03	1.776	1852.
3.	0.294	1590.286	0.157E-03	1.752	2771.
4.	0.356	1586.153	0.156E-03	1.741	3681.
5.	0.417	1583.849	0.156E-03	1.694	5310.
6.	0.398	1563.640	0.150E-03	1.678	7186.
7.	1.113	1586.442	0.156E-03	2.843	1107.
8.	1.085	1586.649	0.156E-03	2.837	1840.
9.	1.110	1585.172	0.156E-03	2.829	2752.
10.	1.201	1576.706	0.154E-03	2.836	5333.
11.	1.284	1574.135	0.153E-03	2.817	7186.
12.	2.286	1578.645	0.154E-03	3.950	1095.
13.	2.309	1579.164	0.154E-03	3.968	1829.
14.	2.345	1582.696	0.155E-03	3.927	2740.
15.	2.376	1579.328	0.154E-03	3.859	3647.
16.	2.418	1575.647	0.153E-03	3.916	5333.
17.	2.319	1572.891	0.153E-03	3.989	7186.
18.	9.162	1564.026	0.149E-03	7.825	1049.
19.	9.236	1560.024	0.147E-03	7.789	1765.
20.	9.090	1556.889	0.147E-03	7.776	2643.
21.	9.095	1551.682	0.145E-03	7.703	3488.
22.	9.451	1555.216	0.144E-03	7.774	5310.
23.	10.396	1554.371	0.144E-03	7.732	7186.
24.	9.946	1556.481	0.144E-03	8.131	1045.

B.4. Test data: Operating conditions and parameters for the Rocketdyne-knurled stator; C_r = .5271 mm.

**ORIGINAL PAGE IS
OF POOR QUALITY**

25.	10. 062	1556. 450	0. 146E-03	B. 101	1744.
26.	10. 087	1558. 357	0. 147E-03	B. 166	2637.
27.	10. 160	1559. 307	0. 147E-03	B. 166	3529.
28.	10. 325	1558. 242	0. 147E-03	B. 156	5310.
29.	11. 470	1557. 100	0. 146E-03	B. 262	7186.
30.	11. 373	1560. 980	0. 147E-03	B. 621	1064.
31.	11. 388	1561. 526	0. 147E-03	B. 608	1765.
32.	11. 400	1563. 281	0. 148E-03	B. 596	2655.
33.	11. 406	1562. 262	0. 148E-03	B. 585	3540.
34.	11. 481	1563. 421	0. 148E-03	B. 570	5310.
35.	11. 268	1551. 510	0. 145E-03	B. 374	7186.

B.4. Test data: Operating conditions and parameters for the Rocketdyne-knurled stator; $C_r = .5271$ mm.

ORIGINAL PAGE IS
OF POOR QUALITY

AXIALLY GROOVED STATOR WITH END SEALS $C_m = 0.8511$ mm
 SEAL TEST HEADER DATA
 DR. D. CHILDS TEXAS A&M OCT. 83

Case	Pa-Pb (Bars)	RHO (Kg/M ³)	MU (N·sec/M ²)	MDOT (Kg/sec)	CPM (Cyc/min)
1.	0.018	1571.695	0.151E-03	1.719	1083.
2.	0.049	1572.114	0.151E-03	1.690	1807.
3.	0.078	1570.459	0.151E-03	1.682	2691.
4.	0.081	1569.126	0.150E-03	1.665	3561.
5.	0.162	1571.176	0.151E-03	1.664	5333.
6.	0.180	1559.462	0.148E-03	1.641	7186.
7.	0.591	1585.743	0.155E-03	2.814	1095.
8.	0.611	1583.991	0.154E-03	2.808	1824.
9.	0.553	1571.409	0.151E-03	2.780	2691.
10.	0.636	1576.865	0.152E-03	2.724	3604.
11.	0.701	1569.733	0.151E-03	2.739	5333.
12.	0.806	1563.735	0.149E-03	2.736	7186.
13.	0.803	1570.823	0.151E-03	3.197	1068.
14.	0.883	1575.302	0.152E-03	3.245	1796.
15.	0.924	1573.107	0.151E-03	3.244	2679.
16.	1.001	1576.515	0.152E-03	3.343	3604.
17.	1.072	1574.748	0.152E-03	3.267	5333.
18.	1.122	1562.144	0.140E-03	3.231	7186.
19.	1.148	1545.346	0.144E-03	3.647	1049.
20.	1.349	1561.697	0.148E-03	3.747	1780.
21.	1.348	1559.440	0.147E-03	3.752	2655.
22.	1.446	1560.759	0.148E-03	3.715	3529.
23.	1.565	1563.114	0.140E-03	3.718	5333.
24.	1.504	1563.236	0.148E-03	3.792	7186.

B.5. Test data: Operating conditions and parameters for the axially-grooved stator; $C_r = .5271$ mm.

ORIGINAL PAGE IS
OF POOR QUALITY

25.	6.348	1564.300	0.149E-03	7.858	1060.
26.	6.395	1565.120	0.149E-03	7.856	1780.
27.	6.371	1560.605	0.140E-03	7.841	2479.
28.	6.424	1560.758	0.148E-03	7.830	3540.
29.	6.621	1559.087	0.147E-03	7.841	5333.
30.	5.757	1570.911	0.151E-03	7.273	7186.
31.	6.924	1562.986	0.149E-03	8.275	1068.
32.	6.998	1565.860	0.149E-03	8.334	1786.
33.	6.947	1563.045	0.149E-03	8.264	2667.
34.	7.108	1565.837	0.150E-03	8.282	3582.
35.	7.199	1559.082	0.147E-03	8.133	5310.
36.	7.732	1569.815	0.150E-03	8.375	7186.
37.	8.630	1571.863	0.151E-03	9.224	1068.
38.	8.726	1572.577	0.151E-03	9.186	1796.
39.	8.713	1570.103	0.150E-03	9.198	2673.
40.	8.860	1573.161	0.151E-03	9.242	3582.
41.	9.168	1571.045	0.150E-03	9.223	5310.
42.	9.531	1573.104	0.151E-03	9.301	7186.
43.	10.390	1565.830	0.149E-03	10.125	1071.
44.	10.478	1570.248	0.150E-03	10.157	1786.
45.	10.461	1565.370	0.148E-03	10.077	2655.
46.	10.386	1562.978	0.148E-03	10.028	3529.
47.	10.454	1559.910	0.147E-03	9.912	5310.
48.	10.707	1571.481	0.150E-03	9.899	7186.

B.5. Test data: Operating conditions and parameters for the axially-grooved stator; $C_r = .5271$ mm.

ORIGINAL PAGE IS
OF POOR QUALITY

DIAMOND GRID STATOR $C_m = 0.8890$ mm
 SEAL TEST HEADER DATA
 DR. D. CHILDS TEXAS A&M OCT. 83

Case	Pa-Pb (Bars)	RHO (Kg/M ³)	MU (N·sec/M ²)	MDOT (Kg/sec)	CPM (Cyc/min)
1.	0. 050	1570. 137	0. 151E-03	1. 671	1087.
2.	0. 084	1567. 164	0. 150E-03	1. 653	1786.
3.	0. 105	1562. 338	0. 149E-03	1. 638	2673.
4.	0. 079	1559. 147	0. 148E-03	1. 614	3529.
7.	0. 884	1562. 381	0. 148E-03	2. 734	1064.
8.	0. 858	1560. 527	0. 148E-03	2. 716	1780.
9.	0. 867	1561. 313	0. 148E-03	2. 706	2667.
10.	0. 870	1558. 118	0. 147E-03	2. 692	3540.
11.	0. 934	1560. 235	0. 148E-03	2. 687	5333.
12.	0. 769	1549. 694	0. 146E-03	2. 651	7186.
13.	1. 826	1557. 954	0. 147E-03	3. 721	1045.
14.	1. 876	1559. 894	0. 147E-03	3. 685	1765.
15.	1. 899	1559. 856	0. 147E-03	3. 711	2643.
16.	1. 929	1560. 030	0. 147E-03	3. 732	3540.
17.	1. 836	1551. 953	0. 145E-03	3. 654	5310.
18.	2. 010	1548. 276	0. 145E-03	3. 722	7186.
19.	8. 708	1552. 463	0. 146E-03	7. 776	1064.
20.	8. 343	1548. 961	0. 145E-03	7. 669	1739.
21.	8. 520	1551. 013	0. 145E-03	7. 742	2620.
22.	8. 217	1543. 646	0. 143E-03	7. 596	3458.
23.	8. 924	1556. 882	0. 147E-03	7. 822	5310.
24.	9. 499	1540. 812	0. 142E-03	7. 656	7186.
25.	9. 712	1569. 259	0. 150E-03	8. 277	1068.
26.	9. 672	1566. 092	0. 149E-03	8. 280	1786.

B.6. Test data: Operating conditions and parameters for the diamond-grid roughened stator; $C_r = .5271$ mm.

ORIGINAL PAGE IS
OF POOR QUALITY

27.	9. 259	1558. 851	0. 147E-03	8. 211	2643.
28.	9. 312	1553. 808	0. 146E-03	8. 150	3519.
29.	9. 327	1552. 247	0. 146E-03	8. 111	5310.
30.	9. 571	1534. 124	0. 141E-03	7. 897	7186.
31.	11. 540	1560. 538	0. 147E-03	8. 900	1053.
32.	11. 277	1553. 383	0. 145E-03	8. 867	1754.
33.	11. 363	1557. 924	0. 146E-03	8. 940	2632.
34.	11. 407	1559. 108	0. 147E-03	8. 933	3519.
35.	11. 466	1557. 539	0. 146E-03	8. 976	5286.
36.	11. 177	1541. 333	0. 142E-03	8. 591	7186.

B.6. Test data: Operating conditions and parameters for the diamond-grid roughened stator; $C_r = .5271$ mm.

DIAMOND GRID STATOR WITH END SEALS $C_m = 0.8164$ mm
 SEAL TEST HEADER DATA
 DR. D. CHILDS TEXAS A&M NOV. 83

Case	Pa-Pb (Bars)	RHO (Kg/M ³)	MU (N·sec/M ²)	MDOT (Kg/sec)	CPM (Cyc/min)
1.	0. 284	1576. 215	0. 152E-03	1. 670	1095.
2.	0. 299	1574. 482	0. 152E-03	1. 691	1802.
3.	0. 293	1570. 882	0. 151E-03	1. 678	2697.
4.	0. 293	1568. 338	0. 150E-03	1. 654	3582.
5.	0. 309	1565. 613	0. 150E-03	1. 681	5310.
6.	0. 299	1546. 517	0. 144E-03	1. 580	7229.
7.	1. 086	1569. 299	0. 151E-03	2. 761	1075.
8.	1. 027	1566. 345	0. 150E-03	2. 723	1791.
9.	1. 079	1567. 327	0. 150E-03	2. 725	2691.
10.	1. 152	1568. 976	0. 151E-03	2. 763	3604.
11.	1. 139	1566. 722	0. 150E-03	2. 744	5333.
12.	1. 057	1553. 684	0. 147E-03	2. 659	7186.
13.	1. 968	1561. 112	0. 140E-03	3. 752	1060.
14.	2. 020	1562. 686	0. 149E-03	3. 754	1780.
15.	2. 077	1564. 875	0. 149E-03	3. 825	2679.
16.	2. 086	1558. 691	0. 140E-03	3. 770	3540.
17.	2. 175	1558. 994	0. 148E-03	3. 786	5333.
18.	2. 079	1556. 244	0. 147E-03	3. 744	7186.
19.	8. 521	1553. 306	0. 146E-03	7. 608	1033.
20.	8. 656	1552. 827	0. 146E-03	7. 614	1749.
21.	8. 405	1549. 605	0. 145E-03	7. 545	2632.
22.	8. 796	1551. 761	0. 145E-03	7. 606	3499.
23.	8. 598	1549. 175	0. 145E-03	7. 549	5310.
24.	9. 342	1554. 166	0. 146E-03	7. 707	7186.

B.7. Test data: Operating conditions and parameters for the diamond-grid roughened stator with end seals; $C_r = .5271$ mm.

25.	11.423	1554.128	0.146E-03	8.823	1056.
26.	11.359	1553.248	0.145E-03	8.771	1744.
27.	11.286	1551.361	0.145E-03	8.778	2609.
28.	11.314	1548.167	0.144E-03	8.671	3468.
29.	11.313	1544.245	0.143E-03	8.750	5310.
30.	11.555	1554.927	0.146E-03	8.616	7186.

B.7. Test data: Operating conditions and parameters for the diamond-grid roughened stator with end seals; $C_r = .5271$ mm.

ROUGH STATOR : HOLE PATTERN 1 C = 0.5080 mm
 SEAL TEST HEADER DATA
 DR. D. CHILDS TEXAS A&M DEC. 83

Case	Pa-Pb (Bars)	RHO (Kg/M ³)	MU (N·sec/M ²)	MDOT (Kg/sec)	CPM (Cyc/min)
1.	0. 620	1552. 474	0. 146E-03	2. 074	1060.
2.	0. 697	1558. 114	0. 147E-03	2. 102	1765.
3.	0. 704	1551. 696	0. 146E-03	2. 074	2626.
4.	0. 790	1554. 577	0. 147E-03	2. 083	3519.
5.	0. 822	1549. 698	0. 145E-03	2. 065	5333.
6.	1. 200	1545. 424	0. 144E-03	2. 035	7186.
7.	1. 725	1554. 154	0. 146E-03	2. 994	1049.
8.	1. 705	1548. 626	0. 145E-03	2. 982	1754.
9.	1. 695	1546. 150	0. 144E-03	2. 971	2603.
10.	1. 738	1546. 850	0. 144E-03	2. 959	3478.
11.	1. 885	1544. 624	0. 144E-03	2. 980	5333.
12.	2. 363	1551. 683	0. 145E-03	3. 006	7186.
13.	2. 736	1551. 120	0. 145E-03	3. 696	1060.
14.	2. 746	1552. 586	0. 146E-03	3. 678	1744.
15.	2. 738	1552. 371	0. 146E-03	3. 673	2632.
16.	2. 865	1555. 686	0. 146E-03	3. 709	3529.
17.	3. 134	1568. 950	0. 150E-03	3. 797	5310.
18.	3. 336	1552. 338	0. 146E-03	3. 740	7186.
19.	12. 118	1550. 553	0. 145E-03	7. 659	1034.
20.	12. 065	1549. 943	0. 144E-03	7. 629	1744.
21.	12. 064	1548. 763	0. 144E-03	7. 664	2597.
22.	12. 068	1546. 753	0. 144E-03	7. 551	3468.
23.	12. 209	1553. 221	0. 145E-03	7. 584	5286.
24.	12. 386	1552. 569	0. 145E-03	7. 057	7186.

B.8. Test data: Operating conditions and parameters for the round-hole-pattern roughened stator; $C_r = .5271$ mm.

SMOOTH STATOR / SMOOTH ROTOR $C = 0.3937$ mm
 SEAL TEST HEADER DATA
 DR. D. CHILDS TEXAS A&M SEP. 83

Case	Ra	CPM (Cyc/min)	Fr/A (MN/M)	dev. (MN/M)	Fo/A (MN/M)	dev. (MN/M)	F (KN)
1.	99987.	1376.	-0.7849	0.1705	0.6262	0.2300	0.0967
2.	100745.	2299.	-0.5787	0.2197	0.7408	0.1378	0.0902
3.	99895.	3109.	-0.3546	0.0981	1.3263	0.1788	0.1331
4.	100727.	3797.	-0.4511	0.1002	1.3527	0.1071	0.1355
5.	100028.	5333.	0.2828	0.1436	1.8039	0.1123	0.1744
6.	100299.	7186.	1.3760	0.1994	2.4489	0.2268	0.2744
7.	149371.	3797.	-1.1154	0.1930	2.5071	0.1354	0.2562
8.	150972.	5310.	-0.2955	0.2232	3.1931	0.1724	0.3046
9.	180214.	1357.	-2.0503	0.1281	1.4539	0.1538	0.2325
10.	180951.	2281.	-1.9358	0.1396	1.9012	0.1346	0.2519
11.	180638.	3117.	-1.5603	0.1264	2.8400	0.1565	0.3032
12.	180861.	7186.	0.2975	0.2293	5.0686	0.3045	0.4858
13.	300052.	1351.	-5.7762	0.3393	2.5121	0.5331	0.5609
14.	299127.	2230.	-5.7842	0.4147	3.6111	0.4162	0.6060
15.	299147.	3158.	-5.7611	0.4164	5.8061	0.3439	0.7272
16.	300914.	3810.	-5.2660	0.2710	6.0631	0.3740	0.7255
17.	299560.	5310.	-3.8651	0.4200	7.7374	0.3966	0.7752
18.	299561.	7186.	-0.8616	0.6023	10.3340	0.4895	0.9281
19.	418111.	1370.	-11.5544	0.5890	3.6755	0.6300	1.0114
20.	414787.	2290.	-12.1084	0.6446	5.8781	0.6777	1.1125
21.	412835.	3109.	-10.9231	0.8073	7.6769	0.5912	1.0905
22.	422988.	3797.	-10.7925	0.7840	10.3884	0.6828	1.2081
23.	415917.	5310.	-8.7813	0.7811	12.5874	0.6602	1.2635

C.1. Test data: Force coefficients (average and standard deviations) and average force magnitude for the smooth stator; $C_r = .3937$ mm.

24. 415388. 7186. -7.2017 0.7691 14.2627 0.7172 1.3253

C.1. Test data: Force coefficients (average and standard deviations)
and average force magnitude for the smooth stator; $C_r = .3937$ mm.

ROCKETDYNE STATOR / SMOOTH ROTOR $C = 0.3937$ mm
 SEAL TEST HEADER DATA
 DR. D. CHILDS TEXAS A&M SEP. 83

Case	Ra	CPM (Cyc/min)	Fr/A (MN/M)	dev. (MN/M)	Fo/A (MN/M)	dev. (MN/M)	IFI (KN)
1.	70483.	1415.	-0. 5820	0. 0656	0. 6866	0. 0645	0. 0835
2.	70111.	2353.	-0. 3413	0. 0851	1. 2121	0. 1006	0. 1166
3.	70090.	3183.	-0. 1945	0. 0597	1. 8175	0. 0795	0. 1674
4.	69845.	3810.	0. 1507	0. 2321	1. 5931	0. 2101	0. 1473
5.	70165.	5333.	1. 1176	0. 1644	2. 3499	0. 1519	0. 2466
6.	69821.	7186.	3. 1332	0. 2603	3. 1594	0. 2386	0. 4253
7.	100320.	1389.	-1. 2155	0. 3630	0. 9173	0. 2346	0. 1422
8.	100160.	2317.	-1. 0595	0. 3276	1. 7110	0. 2811	0. 1866
9.	99869.	3175.	-0. 6638	0. 3032	2. 3271	0. 3753	0. 2282
10.	98995.	3810.	-0. 5267	0. 1212	2. 3704	0. 0969	0. 2257
11.	100670.	5310.	0. 7350	0. 1386	3. 4219	0. 1214	0. 3275
12.	100163.	7186.	2. 5367	0. 3136	4. 3695	0. 2433	0. 4759
13.	119946.	1402.	-1. 8672	0. 0931	1. 2160	0. 0948	0. 2025
14.	119027.	2344.	-1. 4213	0. 2788	2. 0364	0. 1955	0. 2264
15.	120106.	3191.	-1. 2987	0. 1350	3. 0291	0. 1362	0. 3049
16.	119779.	3797.	-0. 9977	0. 2026	3. 1932	0. 1941	0. 3078
17.	120062.	5310.	0. 2463	0. 2801	4. 3109	0. 2948	0. 4001
18.	120825.	7186.	1. 9347	0. 2642	5. 5228	0. 3213	0. 5474
19.	168672.	1376.	-3. 3887	0. 1404	1. 6151	0. 1614	0. 3347
20.	170167.	2290.	-2. 9901	0. 1580	2. 7385	0. 1526	0. 3628
21.	170964.	3125.	-2. 3074	0. 1593	3. 7740	0. 2058	0. 3960
22.	171087.	3810.	-1. 9979	0. 1733	4. 4128	0. 1732	0. 4463
23.	170448.	4919.	-0. 9323	0. 2985	5. 8252	0. 2154	0. 5401
24.	169965.	7186.	0. 9331	0. 3838	8. 0276	0. 3303	0. 7385

C.2. Test data: Force coefficients (average and standard deviations) and average force magnitude for the Rocketdyne-knurled stator;
 $C_r = .3937$ mm.

25.	349280.	1351.	-0. 8563	0. 4343	3. 2233	0. 7160	0. 7956
26.	348162.	2290.	-9. 5218	0. 5223	5. 3797	0. 5364	0. 9088
27.	351452.	3125.	-7. 8221	0. 3645	6. 5922	0. 4881	0. 8606
28.	341701.	3797.	-6. 9158	0. 4196	8. 8296	0. 4359	0. 9323
29.	338284.	5310.	-5. 7545	0. 4766	11. 5694	0. 4904	1. 0666
30.	347042.	7186.	-2. 1525	0. 7269	14. 8202	0. 8005	1. 2504

C.2. Test data: Force coefficients (average and standard deviations) and average force magnitude for the Rocketdyne-knurled stator
 $C_r = .3937$ mm.

SMOOTH STATOR / SMOOTH ROTOR $C = 0.5271$ mm
 SEAL TEST HEADER DATA
 DR. D. CHILDS TEXAS A&M SEP. 83

Case	Ra	CPM (Cyc/min)	Fr/A (MN/M)	dev. (MN/M)	Fo/A (MN/M)	dev. (MN/M)	F (KN)
1.	69823.	1111.	-0.2395	0.0382	0.2361	0.0341	0.0431
2.	70034.	1852.	-0.1724	0.0199	0.4539	0.0363	0.0619
3.	70046.	2771.	0.0422	0.0369	0.5947	0.0452	0.0768
4.	69956.	3681.	0.1607	0.0396	0.3111	0.0542	0.0451
5.	69832.	5310.	1.0270	0.0600	1.0110	0.0592	0.1878
6.	69470.	7186.	2.3604	0.1716	0.8917	0.1567	0.3344
7.	119896.	1083.	-0.3031	0.1004	0.3201	0.1262	0.0632
8.	120532.	1807.	-0.3192	0.0757	0.4187	0.1149	0.0658
9.	120259.	2715.	-0.0040	0.1199	0.7737	0.1541	0.0976
10.	120282	3625.	0.0592	0.0770	0.7285	0.0687	0.0898
11.	119829.	5357.	0.6756	0.1339	0.9281	0.1324	0.1463
12.	119710.	7186.	1.3925	0.1922	1.2926	0.1738	0.2475
13.	170852.	1064.	-0.6714	0.0978	0.4078	0.1259	0.0981
14.	170941.	1744	-0.7867	0.0574	0.8049	0.0677	0.1389
15.	169868.	2620.	-0.4082	0.0998	0.9427	0.0809	0.1284
16.	171628.	3488.	-0.3011	0.1002	0.9881	0.0817	0.1296
17.	169945.	5333.	0.5232	0.1161	1.5273	0.1100	0.2036
18.	170265.	7186.	1.0003	0.1958	2.0193	0.1705	0.3040
19.	270273.	1075.	-1.4779	0.1922	0.9166	0.2893	0.2131
20.	269996.	1780.	-1.6199	0.1323	1.4884	0.1286	0.2659
21.	270083.	2685.	-1.3920	0.1404	1.8098	0.1255	0.2780
22.	270657.	3593.	-0.9201	0.1484	2.2942	0.1335	0.2975
23.	271615.	5333.	-0.0604	0.1368	3.2331	0.1582	0.4004
24.	270589.	7186.	1.4167	0.1853	4.0443	0.2055	0.5398

C.3. Test data: Force coefficients (average and standard deviations)
 and average force magnitude for the smooth stator; $C_r = .5271$ mm.

25.	384629.	1079.	-2.7403	0.2462	1.1100	0.5839	0.3614
26.	384986.	1791.	-3.1715	0.2211	2.1335	0.2547	0.4516
27.	385082.	2679.	-2.9232	0.1722	3.0108	0.2340	0.4995
28.	385101.	3561.	-2.6485	0.3023	3.8099	0.3346	0.5615
29.	385800.	5310.	-1.4494	0.1814	4.9745	0.2789	0.6247
30.	385428.	7186.	0.2633	0.3662	6.9100	0.2878	0.8544
31.	503745.	1056.	-4.9383	0.3523	1.2585	1.1003	0.6018
32.	501772.	1780.	-5.3124	0.4147	2.9234	0.4796	0.7043
33.	500289.	2667.	-5.1237	0.2948	3.7113	0.3275	0.7312
34.	491351.	3561.	-4.5728	0.3248	5.0890	0.3603	0.8007
35.	496088.	5310.	-2.9778	0.3518	6.8597	0.4343	0.8673
36.	481095.	7186.	-0.8457	0.5095	9.4162	0.4115	1.1099
37.	502759.	1053.	-5.0114	0.6367	1.2089	1.0526	0.6150
38.	500662.	1770.	-5.0089	0.3661	2.4911	0.4020	0.6531
39.	503133.	2643.	-4.5297	0.3161	3.5337	0.4658	0.6729
40.	499279.	3550.	-4.4824	0.3940	5.0914	0.3797	0.7876
41.	500366.	5310.	-2.9917	0.4051	7.1481	0.4663	0.9047
42.	498996.	7186.	-2.4883	0.3586	8.2294	0.5249	1.0335

C.3. Test data: Force coefficients (average and standard deviations)
and average force magnitude for the smooth stator; $C_x = .5271$ mm.

ROCKETDYNE STATOR / SMOOTH ROTOR $C = 0.5271$ mm
 SEAL TEST HEADER DATA
 DR. D. CHILDS TEXAS A&M SEP. 83

Case	Ra	CPM (Cyc/min)	F _r /A (MN/M)	dev. (MN/M)	F _o /A (MN/M)	dev. (MN/M)	fF1 (KN)
1.	69823.	1111.	-0.2395	0.0382	0.2361	0.0341	0.0431
2.	70034.	1852.	-0.1724	0.0199	0.4539	0.0363	0.0619
3.	70046.	2771.	0.0422	0.0369	0.5947	0.0452	0.0768
4.	69956.	3681.	0.1407	0.0396	0.3111	0.0542	0.0451
5.	69832.	5310.	1.0270	0.0600	1.0110	0.0592	0.1878
6.	69470.	7186.	2.3604	0.1716	0.8917	0.1567	0.3344
7.	115592.	1107.	-0.7311	0.0896	0.4581	0.1277	0.1091
8.	115601.	1840.	-0.6153	0.1172	0.8831	0.1251	0.1361
9.	115059.	2752.	-0.2842	0.1731	1.1645	0.1245	0.1552
10.	115312.	5333.	0.6568	0.1447	1.5408	0.1181	0.2180
11.	116790.	7186.	2.4329	0.1498	1.7780	0.1942	0.4093
12.	160632.	1095.	-1.3730	0.0998	0.5339	0.2297	0.1866
13.	160365.	1829.	-1.1773	0.1153	1.1165	0.0633	0.2034
14.	159885.	2740.	-0.8076	0.1195	1.5866	0.1182	0.2232
15.	160001.	3647.	-0.9083	0.0653	1.5632	0.0786	0.2348
16.	159908.	5333.	0.2738	0.1193	2.2919	0.0879	0.2971
17.	160331.	7186.	2.1398	0.1565	3.0330	0.1468	0.4810
18.	336188.	1049.	-4.8603	0.4263	1.2325	0.9696	0.6248
19.	335555.	1765.	-4.8769	0.1845	2.2804	0.1983	0.6543
20.	334650.	2643.	-4.5587	0.1414	2.9544	0.1192	0.6625
21.	336486.	3488.	-3.9449	0.2648	3.8485	0.2514	0.6651
22.	335621.	5310.	-2.5291	0.2813	5.5779	0.2561	0.7583
23.	335240.	7186.	-0.7753	0.3018	8.3946	0.2673	1.0421
24.	350174.	1045.	-5.2278	0.3886	1.3552	1.0481	0.6691

c.4. Test data: Force coefficients (average and standard deviations) and average force magnitude for the Rocketdyne-knurled stator;
 $C_r = .5271$ mm.

25.	350214.	1744.	-5. 0409	0. 1669	2. 1450	0. 2024	0. 6653
26.	350986.	2637.	-5. 0585	0. 1597	3. 0642	0. 2458	0. 7220
27.	349829.	3529.	-4. 5195	0. 1763	3. 8877	0. 3332	0. 7302
28.	350373.	5310.	-2. 5727	0. 2406	5. 8553	0. 3390	0. 7848
29.	351413.	7186.	-1. 2351	0. 2694	9. 0472	0. 3020	1. 1173
30.	367565.	1064.	-6. 0722	0. 3615	1. 0398	1. 1891	0. 7496
31.	370081.	1765.	-5. 8171	0. 2272	2. 6012	0. 2447	0. 7648
32.	368824.	2655.	-6. 0132	0. 3081	3. 5672	0. 3143	0. 8385
33.	367794.	3540.	-4. 8014	0. 1800	4. 6171	0. 2282	0. 8036
34.	367890.	5310.	-3. 0625	0. 2945	6. 7035	0. 3136	0. 8863
35.	367212.	7186.	-0. 6234	0. 3338	8. 6858	0. 3952	1. 0745

C.4. Test data: Force coefficients (average and standard deviations) and average force magnitude for the rocketdyne-knurled stator;
 $C_r = .5271$ mm.

AXIALLY GROOVED STATOR WITH END SEALS $C_{rr} = 0.8511$ mm
 SEAL TEST HEADER DATA
 DR. D. CHILDS TEXAS A&M OCT. 83

Case	Ra	CPM (Cyc/min)	Fr/A (IN/M)	dev. (MN/M)	Fo/A (MN/M)	dev. (MN/M)	F (kN)
1.	69887.	1083.	-0.0652	0.0747	0.2107	0.0557	0.0294
2.	69729.	1807.	-0.0013	0.0720	0.3408	0.0697	0.0437
3.	70053.	2691.	0.2190	0.0459	0.5153	0.0844	0.0720
4.	70106.	3561.	0.3015	0.0574	0.3885	0.0798	0.0627
5.	69489.	5333.	1.2925	0.1541	0.9387	0.1441	0.2051
6.	70005.	7186.	2.8412	0.1428	0.4755	0.1378	0.3808
7.	114895.	1095.	-0.1643	0.1082	0.4032	0.0945	0.0562
8.	114806.	1824.	0.0018	0.0758	0.7594	0.0964	0.0951
9.	115138.	2671.	0.2438	0.0801	0.9877	0.0744	0.1305
10.	115006.	3604.	0.3191	0.1169	0.8882	0.1117	0.1185
11.	115477.	5333.	1.2995	0.0870	1.5569	0.0785	0.2609
12.	115272.	7186.	2.8402	0.1023	1.5103	0.1135	0.4199
13.	135289.	1068.	-0.1708	0.1220	0.4938	0.0648	0.0678
14.	135554.	1796.	0.0416	0.0749	0.7890	0.0734	0.0789
15.	135061.	2679.	0.2689	0.0478	1.1768	0.0753	0.1524
16.	135148.	3604.	0.3011	0.0790	1.3151	0.0907	0.1678
17.	134715.	5333.	1.4079	0.1313	1.0465	0.1073	0.2952
18.	138136.	7186.	2.9906	0.1367	1.9848	0.1575	0.4691
19.	160348.	1049.	-0.1069	0.0983	0.5420	0.0937	0.0737
20.	160409.	1780.	-0.3426	0.0692	1.0638	0.0842	0.1400
21.	160387.	2655.	0.1208	0.0504	1.2739	0.1043	0.1621
22.	159505.	3529.	0.2011	0.1194	1.5135	0.1025	0.1924
23.	160464.	5333.	1.3978	0.0937	2.2230	0.0724	0.3348
24.	159919.	7186.	3.1055	0.1395	2.4067	0.1284	0.5133

C.5. Test data: Force coefficients (average and standard deviations) and average force magnitude for the axially-grooved stator;
 $C_{rr} = .5271$ mm.

25.	334987.	1060.	-1. 0799	0. 2498	0. 8457	0. 2777	0. 1740
26.	334990.	1780.	-1. 1060	0. 0742	2. 1289	0. 0800	0. 2929
27.	334706.	2479.	-0. 6817	0. 0767	2. 6464	0. 1006	0. 3402
28.	335005.	3540.	-0. 3002	0. 1564	3. 7084	0. 1585	0. 4514
29.	335174.	5333.	1. 4125	0. 1649	5. 2658	0. 1411	0. 6781
30.	300004.	7186.	3. 4754	0. 1610	6. 4689	0. 2395	0. 9251
31.	350805.	1068.	-1. 0090	0. 3418	1. 0518	0. 2210	0. 2101
32.	349862.	1786.	-1. 2694	0. 1339	2. 1738	0. 1225	0. 3060
33.	349247.	2667.	-0. 6044	0. 1297	3. 2692	0. 3244	0. 4077
34.	349922.	3582.	-0. 1092	0. 1005	3. 7495	0. 1324	0. 4506
35.	349818.	5310.	1. 2781	0. 2063	5. 5141	0. 2020	0. 7026
36.	349680.	7186.	3. 1860	0. 1989	7. 6815	0. 1851	1. 0371
37.	385150.	1068.	-2. 0301	0. 3168	1. 1072	0. 4685	0. 2903
38.	385647.	1796.	-1. 8653	0. 1826	2. 2402	0. 1584	0. 3546
39.	385493.	2673.	-1. 3307	0. 1685	3. 3181	0. 2340	0. 4392
40.	385238.	3582.	-0. 7917	0. 2612	4. 6181	0. 1603	0. 5817
41.	384755.	5310.	0. 5797	0. 2426	6. 7398	0. 2639	0. 8299
42.	384523.	7186.	3. 3940	0. 2420	8. 6242	0. 1935	1. 1416
43.	428167.	1071.	-2. 0995	0. 4505	1. 0350	0. 4547	0. 2911
44.	427833.	1786.	-1. 5471	0. 1849	2. 3334	0. 2700	0. 3380
45.	427999.	2655.	-1. 2443	0. 3240	3. 7053	0. 2437	0. 4746
46.	430603.	3529.	-0. 7400	0. 3465	4. 7549	0. 1149	0. 5965
47.	425806.	5310.	1. 1046	0. 2286	7. 1480	0. 3008	0. 0817
48.	406211.	7186.	3. 3347	0. 2366	9. 2456	0. 2108	1. 2017

C.5. Test data: Force coefficients (average and standard deviations) and average force magnitude for the axially-grooved stator;
 $C_x = .5271$ mm.

DIAMOND GRID STATOR $C_m = 0.8890$ mm
 SEAL TEST HEADER DATA
 DR. D. CHILDS TEXAS A&M OCT. 83

Case	Ra	CPM (Cyc/min)	Fx/A (MN/M)	dev. (MN/M)	Fy/A (MN/M)	dev. (MN/M)	F (kN)
1.	70269.	1087.	-0.0700	0.1186	0.1509	0.0932	0.0268
2.	70522.	1786.	0.0468	0.0814	0.3423	0.0841	0.0447
3.	69958.	2673.	0.1695	0.1229	0.4588	0.1685	0.0643
4.	70567.	3529.	0.0601	0.1188	0.4024	0.1013	0.0536
7.	115392.	1064.	-0.1979	0.0816	0.3356	0.1151	0.0500
8.	114981.	1780.	-0.0978	0.0871	0.5165	0.0575	0.0670
9.	114309.	2667.	0.0706	0.0463	0.7165	0.0815	0.0911
10.	115239.	3540.	0.0120	0.1095	0.9018	0.1238	0.1180
11.	115493.	5333.	0.7848	0.0763	1.1012	0.0805	0.1731
12.	115107.	7186.	1.7903	0.2503	1.0037	0.1985	0.2694
13.	159903.	1045.	-0.3967	0.1430	0.4154	0.1599	0.0756
14.	160021.	1765.	-0.2066	0.1059	0.8711	0.0755	0.1153
15.	159704.	2643.	-0.2229	0.1702	1.2697	0.2142	0.1653
16.	159925.	3540.	-0.0987	0.1178	1.3874	0.1317	0.1738
17.	159456.	5310.	0.8027	0.1063	1.6267	0.0873	0.2393
18.	160083.	7186.	2.0102	0.2089	1.6690	0.1303	0.3394
19.	335721.	1064.	-1.4822	0.1680	0.7621	0.3839	0.2216
20.	335593.	1739.	-1.4436	0.1448	1.8155	0.1503	0.2846
21.	335547.	2620.	-1.3300	0.0771	2.4416	0.1016	0.3441
22.	335436.	3458.	-1.1291	0.1845	3.3268	0.2242	0.4307
23.	335895.	5310.	-0.0929	0.2627	4.0987	0.2153	0.6063
24.	335547.	7186.	1.5237	0.2614	5.6586	0.2674	0.7387
25.	349557.	1068.	-1.6831	0.2575	0.9574	0.5451	0.2470

C.6. Test data: Force coefficients (average and standard deviations) and average force magnitude for the diamond-grid roughened stator; $C_r = .5271$ mm.

26.	351361.	1786.	-1.5493	0.1690	2.3387	0.1085	0.3444
27.	349769.	2643.	-1.4850	0.1238	2.9625	0.0907	0.4123
28.	349793.	3519.	-1.4175	0.1024	3.6328	0.1691	0.4863
29.	350527.	5310.	-0.2060	0.2199	5.0063	0.1743	0.6217
30.	348392.	7186.	2.1179	0.2975	5.5752	0.3634	0.7587
31.	382545.	1053.	-1.9834	0.2789	0.9390	0.5207	0.2755
32.	384953.	1754.	-1.9781	0.1816	2.4619	0.3185	0.3854
33.	386286.	2632.	-2.0234	0.1364	3.3541	0.3130	0.4033
34.	381826.	3519.	-1.5984	0.3427	3.8194	0.3341	0.5186
35.	385294.	5286.	0.0382	0.2803	5.6084	0.2655	0.4980
36.	382785.	7186.	1.8587	0.2722	6.2719	0.3277	0.8163

C.6. Test data: Force coefficients (average and standard deviations) and average force magnitude for the diamond-grid roughened stator; $C_r = .5271$ mm.

DIAMOND GRID STATOR WITH END SEALS $C_m = 0.8164$ mm
 SEAL TEST HEADER DATA
 DR. D. CHILDS TEXAS A&M NOV. 83

Case	Ra	CPM (Cyc/min)	F _r /A (MN/M)	dev. (MN/M)	F _a /A (MN/M)	dev. (MN/M)	F (KN)
1.	70086.	1095.	-0.0977	0.0727	0.2112	0.0703	0.0310
2.	70004.	1802.	0.0667	0.0781	0.4155	0.0374	0.0538
3.	70092.	2697.	0.1085	0.0380	0.4720	0.0611	0.0617
4.	70028.	3582.	0.1177	0.1477	0.6491	0.1571	0.0866
5.	69906.	5310.	0.8566	0.0749	0.8753	0.0420	0.1579
6.	70014.	7229.	1.4095	0.2512	0.5831	0.2712	0.2137
7.	115291.	1075.	-0.2167	0.2039	0.4641	0.1226	0.0689
8.	115305.	1791.	0.1675	0.1012	0.7296	0.0817	0.0948
9.	114956.	2691	0.2118	0.1658	1.2736	0.2137	0.1669
10.	115498.	3604.	0.1793	0.1003	1.2010	0.0822	0.1497
11.	115384.	5333.	0.8527	0.3818	1.5465	0.3954	0.2310
12.	114385.	7186.	1.6584	0.2256	1.6649	0.3372	0.3090
13.	159172.	1060.	-0.4374	0.1355	0.5855	0.0891	0.0931
14.	160206.	1780.	-0.4456	0.1184	1.0633	0.1000	0.1458
15.	159976.	2679.	0.0439	0.1030	1.3595	0.0518	0.1731
16.	159452.	3540.	0.2313	0.0780	1.6308	0.0931	0.2053
17.	159868.	5333.	0.8550	0.1385	2.2625	0.1331	0.3103
18.	159580.	7186.	1.9449	0.2128	2.1949	0.2009	0.3932
19.	325877.	1053.	-1.7079	0.2492	0.8620	0.3947	0.2412
20.	330705.	179.	-1.9614	0.1727	2.1456	0.2244	0.3567
21.	330605.	2332.	-1.2956	0.1319	2.8940	0.1333	0.3939
22.	329749.	3499.	-0.9677	0.2551	3.9808	0.2457	0.4933
23.	330503.	5310.	0.7397	0.2889	5.3616	0.3086	0.6768
24.	330490.	7186.	3.3939	0.3364	7.0800	0.2616	0.9884

C.7. Test data: Force coefficients (average and standard deviations) and average force magnitude for the diamond-grid roughened stator with end seals; $C_r = .5271$ mm.

25.	380534.	1056.	-2. 3241	0. 3549	1. 0433	0. 6482	0. 3210
26.	382526.	1744.	-2. 0791	0. 3347	2. 3181	0. 2305	0. 3803
27.	381068.	2609.	-2. 1704	0. 2229	3. 3490	0. 3476	0. 4940
28.	380551.	3468.	-1. 4770	0. 1805	4. 5471	0. 2346	0. 5752
29.	385017.	5310.	0. 1742	0. 3813	5. 8827	0. 2954	0. 7254
30.	375819.	7186.	3. 5152	0. 3177	8. 2254	0. 3626	1. 1043

C.7. Test data: Force coefficients (average and standard deviations) and average force magnitude for the diamond-grid roughened stator with end seals; $C_r = .5271$ mm.

ROUGH STATOR : HOLE PATTERN I $C = 0.5080$ mm
 SEAL TEST HEADER DATA
 DR. D. CHILDS TEXAS A&M DEC. 83

Case	Ra	CPM (Cyc/min)	Fr/A (MN/M)	dev. (MN/M)	Fo/A (MN/M)	dev. (MN/M)	F (KN)
1.	90081.	1060.	-0.3425	0.1142	0.4400	0.1030	0.0726
2.	87269.	1765.	-0.2850	0.0537	0.8891	0.0704	0.1168
3.	90287.	2626.	-0.0707	0.0532	1.0708	0.0566	0.1347
4.	90691.	3519.	0.1101	0.0627	1.5963	0.0405	0.1998
5.	89609.	5333.	0.7439	0.1432	2.1593	0.1051	0.2931
6.	88551.	7186.	1.9980	0.4122	1.6380	0.3673	0.3429
7.	129806.	1049.	-0.7626	0.1720	0.7203	0.1723	0.1336
8.	130709.	1754.	-0.7114	0.1065	1.1838	0.0763	0.1733
9.	130627.	2603.	-0.5059	0.0794	1.6455	0.1267	0.2157
10.	130816.	3478.	-0.0197	0.0717	2.2152	0.1191	0.2765
11.	129497.	5333.	0.3767	0.1869	3.0220	0.1295	0.3900
12.	130819.	7186.	1.7450	0.2691	3.1921	0.3392	0.4750
13.	160279.	1060.	-1.1806	0.1962	0.9126	0.2619	0.1890
14.	160689.	1744.	-1.1525	0.1690	1.4742	0.1378	0.2328
15.	159279.	2632.	-0.7366	0.0969	2.1330	0.0932	0.2829
16.	159801.	3529.	-0.5044	0.1530	2.9671	0.1600	0.3872
17.	159903.	5310.	0.4026	0.1665	3.9076	0.1545	0.4960
18.	158409.	7186.	1.7762	0.2725	4.1801	0.3156	0.5877
19.	335238.	1034.	-5.1036	0.4935	1.7302	1.0361	0.6649
20.	334707.	1744.	-4.8976	0.3017	3.2653	0.1996	0.7002
21.	336938.	2597.	-4.5033	0.3621	4.9820	0.2974	0.8027
22.	331552.	3468.	-3.8063	0.2146	6.0478	0.1967	0.8557
23.	325604.	5286.	-1.9258	0.3734	8.7138	0.3726	1.0697
24.	306583.	7186.	0.1359	0.3688	11.5721	0.4461	1.3705

C.8. Test data: Force coefficients (average and standard deviations) and average force magnitude for the round-hole-pattern stator;
 $C_r = .5271$ mm.